

---

Theses and Dissertations

---

Summer 2016

## Quantitative analysis in energy loss and vertical mass transport of various channel restoration structures using physical based modeling

Katie May Snyder  
*University of Iowa*

Follow this and additional works at: <https://ir.uiowa.edu/etd>



Part of the [Civil and Environmental Engineering Commons](#)

Copyright © 2016 Katie May Snyder

This thesis is available at Iowa Research Online: <https://ir.uiowa.edu/etd/2144>

---

### Recommended Citation

Snyder, Katie May. "Quantitative analysis in energy loss and vertical mass transport of various channel restoration structures using physical based modeling." MS (Master of Science) thesis, University of Iowa, 2016.

<https://doi.org/10.17077/etd.bpvta68n>

---

Follow this and additional works at: <https://ir.uiowa.edu/etd>



Part of the [Civil and Environmental Engineering Commons](#)

**QUANTITATIVE ANALYSIS IN ENERGY LOSS AND VERTICAL MASS  
TRANSPORT OF VARIOUS CHANNEL RESTORATION STRUCTURES USING  
PHYSICAL BASED MODELING**

By

Katie May Snyder

A thesis submitted in partial fulfillment  
of the requirements for the Master of Science degree  
in Civil and Environmental Engineering  
in the Graduate College of  
The University of Iowa

August 2016

Thesis Supervisor: Professor A. Jacob Odgaard

Copyright by  
KATIE MAY SNYDER

2016

All Rights Reserved

Graduate College  
The University of Iowa  
Iowa City, Iowa

CERTIFICATE OF APPROVAL

---

MASTER'S THESIS

---

This is to certify that the Master's thesis of

Katie May Snyder

has been approved by the Examining Committee for the  
thesis requirement for the Master of Science degree in  
Civil and Environmental Engineering at the August 2016 graduation.

Thesis Committee:

\_\_\_\_\_  
A. Jacob Odgaard, Thesis Supervisor

\_\_\_\_\_  
Corey Markfort

\_\_\_\_\_  
Larry J. Weber

## ACKNOWLEDGMENTS

This thesis would not be possible without the assistance and guidance from Professor A. Jacob Odgaard. I am grateful for the opportunity to continue research on his patented “Iowa Vanes”, to investigate their applications and limitations compared to other commonly used channel restoration technologies, and to present our findings to fellow colleges at the World Environmental & Water Resources Congress and River Flow 2016 conferences. The following consists of meticulously investigated experiments performed by the author, with unbiased data collection and analysis, in order to improve the efficiency of existing channel restoration structure design with emphasis on flood mitigation and re-aeration. Findings should serve as initiative for future research in the technological development and solutions in the field of channel restoration. Integration in the disciplines of environmental and resources engineering, eco-hydraulics, and stream and watershed hydrology is strongly urged by Professor Odgaard and myself for a holistic resolution to our water quality and quantity issues. It is to my great pleasure that I was able to be a part of this journey.

## ABSTRACT

Physical based modeling was conducted to improve channel restoration efforts through direct comparison of submerged structures of various design and orientations. In-stream structure technologies studied are used to provide bank stabilization, flow control, scour and sediment control, as well as ecological enhancement through turbulent dispersion and vertical mass transport. Quantitative analysis evaluates flow effects induced by common channel restoration structures in their ability to provide mixing in our streams and rivers without significant impacts on flooding through excessive energy loss and backwater effect. Physical, fixed-bed flume experiments were performed under high-Reynolds number subcritical steady-state flow conditions. Theoretical energy loss relationships were developed, compared, and evaluated experimentally for stream barbs, spurs, submerged vanes, blocks and boulders. Extensive surface dye-trace experiments were performed to determine centerline mixing and vertical mass transport produced by stream barbs, vanes and boulders. The research presented in this thesis illustrates that the use of dispersion relationships to assess length of vertical mass transport based on the change in energy slope, and estimated shear velocity, of the channel does not properly correct for boundary layer formation and advection or angular motion produced by channel restoration structures. Submerged vanes were found to provide efficient vertical mixing with minimal energy loss or flood risk, as compared to stream barbs, spurs, blocks, and boulders. The deterioration of water quality and the need to provide bank stabilization with limited flood risk require updated NRCS and ASCE design standards and selection tools for vertical mass transport and energy loss relationships of channel restoration structures. The research conducted in these two studies have provided data for a select number of such structures.

## PUBLIC ABSTRACT

Restoration and rehabilitation of streams and rivers include use of submerged structures that provide bank protection, flow training, scour and sediment control, along with turbulent mixing. A lack of engineering design guidelines results in high failure rate, limited ecological improvement, and excessive flow resistance leading to backwater effect and increased flooding risk. Climate change with increased large storm events and continued deterioration of water quality provide a new perspective in eco-hydraulics to couple biology and hydrodynamics for in-stream restoration technologies. In this study we examine channel restoration structures that deliver flood mitigation and water quality enhancement through vertical mass transport. In physical based modeling we compare energy loss and backwater effects associated with common restoration structures (stream barbs, spurs, vanes, blocks, and boulders) to their ability to provide complete vertical mixing. Results show that submerged vanes offer bank stabilization with similar energy loss or backwater effect compared to stream barbs, with more effective vertical mixing. Boulders, large stream barbs, spurs and blocks showed significant backwater effect with limited vertical mass transport.

## TABLE OF CONTENTS

LIST OF TABLES .....	vi
LIST OF FIGURES .....	vii
LIST OF NOTATIONS .....	x
LIST OF ABBREVIATIONS.....	xii
Chapter 1. Introduction .....	1
1.1 Background.....	1
1.2 Research Statement.....	2
1.3 Thesis Organization .....	3
Chapter 2. Channel Restoration Structures.....	4
2.1 Stream Barbs.....	4
2.2 Submerged Vanes .....	5
2.3 Boulders .....	7
Chapter 3. Energy Loss and Backwater Effect Study.....	9
3.1 Introduction.....	9
3.2 Energy Loss Theory .....	10
3.3 Methods.....	15
3.4 Backwater Effect (BWE) Experimental Procedure .....	16
3.5 Results.....	18
3.6 Summary.....	23
Chapter 4. Vertical Mass Transport Study.....	25
4.1 Introduction.....	25
4.2 Open Channel Mixing Theory .....	26
4.3 Method .....	28
4.4 Vertical Mass Transport (VMT) Experimental Procedure .....	28
4.5 Results.....	30
4.6 Summary .....	35
Chapter 5. Conclusions, Engineering Significance, and Future Research.....	36
5.1 Energy Loss and Vertical Mass Transport Study Conclusions.....	36
5.2 Engineering Significance .....	39
5.3 Future Research .....	40
References.....	42
Appendix A. Physical Model Diagrams and Pictures.....	46
A.1 Titled Flume.....	46
A.2 Channel Restoration Structure Design.....	48
A.3 Vertical Mass Transport.....	57
Appendix B. Experimental Data.....	59
B.1 Backwater Effect and Energy Loss Measurements.....	59
B.2 Vertical Mass Transport and Dye Trace Measurements .....	61



## LIST OF TABLES

Table 1. Backwater effect and energy loss on channel restoration structures .....	17
Table 2. Backwater effect measurements compared to theoretical values. ....	19
Table 3. Vertical mass transport and mixing study with channel restoration structures...	29
Table 4. Increase in vertical velocity (VMT) compared to estimated energy loss (BWE).....	37
Table 5. Shear velocity, vertical diffusivity, and length of vertical mass transport compared to experimental measurements.....	38
Table B-1. BWE change in depth in inches for submerged vanes, 11 sets.....	59
Table B-2. BWE change in depth in inches for vane and vane equivalents. ....	59
Table B-3. BWE change in depth in inches for bank attached structures.....	59
Table B-4. BWE change in depth in inches for side wall ramp systems .....	60
Table B-5. BWE change in depth in inches for boulder system.....	60
Table B-6. VMT data for structures flow conditions of 0.8 ft/s velocity and 8-inch water depth.....	61
Table B-7. Submergence ratio VMT data for structures flow conditions of 0.8 ft/s velocity and at different water depths.....	62

## LIST OF FIGURES

Figure 1. USDA Design of a Stream Barb, 2013.....	5
Figure 2. Single submerged vane induced vortices (Top) and array of vanes inducing counterclockwise mixing, Odgaard, 2009. ....	6
Figure 3. Boulder cluster design by NRCS, NEH, 1998. ....	7
Figure 4. Backwater effect measurements by different vane orientations, at 0 to 25 degrees in 5 degree increments, with 5 vanes array field of 11. ....	20
Figure 5. Backwater effect measurements by different number of vane arrays. ....	20
Figure 6. Backwater effect by vane system compared to frontal projections and full blocks, at 10, 20 and 25 degrees. ....	21
Figure 7. Backwater effect by stream barb, spur and vane attached systems. ....	21
Figure 8. Backwater effect by boulder system.....	22
Figure 9. Preliminary dye-trace study with submerged vane array. ....	30
Figure 10. Increase in vertical velocity for single submerged vane array at various orientations.....	32
Figure 11. Increase in vertical velocity for two vane array system. ....	32
Figure 12. Increase in vertical velocity for single stream barb array.....	33
Figure 13. Increase in vertical velocity for boulders at various layouts. ....	33
Figure 14. Submergence ratio effects on the increase in vertical velocity for submerged vane structures. ....	34
Figure A-1. IIHR's Tilted flume, a three-foot-wide rectangular flume with length of 54 feet.....	46
Figure A-2. Plane view of experimental set-up on IIHR's Tilted Flume. ....	46
Figure A-3. Laboratory experimental set-up of backwater effect measurement devices (Left) and vertical mass transport dye tracer device (Right). ....	47
Figure A-4. Flume sheeted covering and lining system utilized in vertical mass transport dye tracer investigations. ....	47

Figure A-5. Backwater and vertical mass transport plan and elevation diagram for stream barb ( $H=d/2 = 4$ -inches shown). Both designs angled at 27 degrees.....	48
Figure A-6. Plan view of actual stream barb structures, small stream barb and large stream barb.....	49
Figure A-7. Stream Barb array used in backwater effect study.....	49
Figure A-8. Backwater study plan and elevation diagram spur ( $H=d/2 = 4$ -inches shown). Structures are angled at 27 degrees into the direction of flow.....	50
Figure A-9. Spur array used in backwater effect study. ....	50
Figure A-10. Vane – wall structure backwater study plan and elevation diagram. Structures are angled at 20 degrees into the direction of flow.....	51
Figure A-11. Vane – wall system used in backwater effect study, angled at 20-degrees. Also known as the vane spur combination. Note: Picture taken from downstream looking upstream.....	51
Figure A-12. Plan view of metal vane - ramp system used in backwater effect study.....	52
Figure A-13. Metal vane – ramp system used in backwater effect study.....	52
Figure A-14. Metal vane array structure backwater and vertical mass transport plan and elevation diagram.....	53
Figure A-15. Plan view of metal vane and block equivalents given angle of attack.....	53
Figure A-16. Metal vane and equivalent full block and frontal projections used in backwater effect study. ....	54
Figure A-17. Boulders or hemisphere blocks used in backwater effect study.....	55
Figure A-18. Two boulder array structure backwater study plan and elevation diagram. ....	56
Figure A-19. Boulder structure used in backwater effect and vertical mass transport study.....	56
Figure A-20. Boulder, marbles covered naturalized vane and metal vane structures.....	57
Figure A-21. Small and large stream barb structures. ....	57

Figure A-22. Vertical mass transport study; boulder design orientations, including (Top) two arrays of single boulders, two arrays of two boulders angles at 45-degrees, (Bottom) single boulder, and 4 boulder cluster. .... 58

## LIST OF NOTATIONS

$A_p$	Stream wise projected area of the structure
$\alpha$	Structure angle of attack with the flow
$b$	Channel or flume width
$c_D$	Drag coefficient
$c_L$	Lift coefficient
$d$	Depth of flow
$d/H$	Submergence ratio
$\Delta d$	Change in the depth of flow
$\varepsilon$	Eddy viscosity
$e$	Submerge vane efficiency number
$F_D$	Structure-induced drag force
$F_L$	Structure-induced lift force
$g$	Acceleration due to gravity
$H$	Height of structure
$H/L$	Aspect ratio
$\kappa$	von Karmon constant ( $\sim 0.40$ )
$L$	Length of structure
$L_x$	Length of vertical mass transport
$\ell$	Longitudinal distance between upstream and downstream section
$N$	Number of structures in system
$\rho$	Water density
$Q$	Flow rate
$S_f$	Slope of friction
$S_o$	Slope of channel
$\Delta S$	Change in slope of channel
$\Gamma$	Structure-induced horizontal circulation
$\tau$	Shear stress
$u$	Average steady flow velocity
$u^*$	Shear velocity

$\Delta u_z$	Increase in vertical velocity
$u_z$	Average vertical velocity
$\nu$	Dynamic viscosity
$\nu$	Viscosity
$W$	Width of structure
$w$	Width of channel

## LIST OF ABBREVIATIONS

B	Boulder
BL	Block
BWE	Backwater effect
FP	Frontal Projections
MV	Metal Vane
R-MV	Rock covered metal vane
S	Spur
SB	Stream Barbs
VMT	Vertical mass transport

# CHAPTER 1.

## INTRODUCTION

Channel restoration frequently utilize in-stream structures designed to provide flow modification, bank stabilization, manage geomorphology, navigation and habitat diversity. To a lesser extent structures may be employed to induce turbulence mixing and vertical mass transport. The need to improve water quality, protect against high storm events, and provide flow control or flood mitigation however require a reevaluation of traditional restoration structures. The goal of this study is to improve channel restoration efforts through quantitative analysis and comparison the ability of existing restoration technologies to provide mixing in our streams and rivers without significant impacts on flooding through excessive energy loss and backwater effect.

### 1.1 Background

Surface waters have played a pivotal role throughout the history of civilization. Channelization, stream alteration, flow control, as well as improved navigation and water transport have resulted in economic, social, and environmental advances for mankind. The predominant focus of channel restoration projects has been to maintain flow dynamics for navigation or water transport, as well as control of bank stability, sediment transport, and scouring of natural or manmade rivers (Maddock, 2013). Modern rehabilitation efforts have been engineered to minimize the negative consequences from channelizing and damming of rivers. Focus on geomorphology and rehabilitation provide effective stream stabilization and ecological improvements (Small, 2012). Despite the popularity of channel restoration many projects have low levels of effectiveness and life span due to poor design or construction (Radspinner, 2009). A nationwide investigation of the restoration projects in the National River Restoration Science Synthesis (NRRSS) database found that only 10% of projects provide initiative for assessment or monitoring after completion. High profile projects were often focused on reconnected floodplains, modification of flow, improvements to aesthetics and recreation, or reconfiguration of channel. Conversely 20% of the total 37,099 projects had no outlined goals (Bernhardt,



2005). Recent reviews in geomorphology, stream characterization and stream restoration ‘art’ have recently been criticized for general conclusions and assumptions with limited *science* in design practices (Small, 2012; Palmer 2014). Additionally, energy loss associated with the introduction of submerged channel structures have become a greater concern not properly assessed in design of many projects around the world. As a consequence, such technologies exhibit excessive energy loss causing backwater and increase flood occurrence and/or stage. Backwater effect has been seen through the use of groynes and dikes. Most notably in Europe and along the Mississippi River, as reviewed by the Army Corps of Engineers (2014) and Hossein Azinfar (2011).

The negative effects of increased flooding, backwater, and headloss through the use of popular bank stability structures has counteracted channel restoration efforts, including such attempts for water quality and ecological enhancement. The work by Robert Ryan Radspinner (2009) offer the most extensive review on restoration flow control structures and projects, in effort to advance traditional design guidelines to combat channel restoration projects’ high failure rate. Numerical evaluation and modeling have traditionally been performed on a single restoration structure, often compared to flume experiments and validated. Yet, no known studies have been performed to examine a wide variety of structure design and orientations for backwater effect or energy loss.

## **1.2 Research Statement**

The research conducted for this thesis is the first of its kind to conduct an extensive evaluation through physical models on popular channel restoration structures such as stream barbs, spurs, submerged vanes, and boulders using NRCS and ASCE design standards. Tests were conducted under steady subcritical flow conditions for *both* backwater effect and vertical mass transport. It is to be noted that research performed to determine a channel restoration structure ability to produce excessive headloss or a backwater effect have recently been criticized by the Army Corps of Engineers. The following research, utilizing a fixed bed rectangular flume, cannot properly correct for scour and or streambed morphology that often develop around in-stream structures. The

methodology used to quantify the differences in structure selection, design, and orientation are not meant to be inclusive. Nevertheless, it is an initial stage performed with the goal of identifying the general nature of restoration structures. Due to the large number of energy loss and vertical mass transport investigations, comparisons under varying flow conditions were not feasible during these two studies. Thus physical based modeling have largely been carried out under a single flow condition. The research objective in this thesis is to perform extensive physical based experiments on existing channel restoration structures as well as several new or combined systems to assist in the identification of efficient structure design and or orientation to minimize flooding risk. The impact of channel restoration structures on vertical mass transport found in this study suggest additional design considerations not currently outlined in design manuals. Experimental observations presented in this thesis provide deeper understanding into the nature of channel restoration structures ability to cause energy loss and vertical mixing by advection, vorticity, and turbulence.

### **1.3 Thesis Organization**

This thesis encompasses two independent physical based studies performed on various channel restoration structures and conducted in a rectangular fixed bed flume. Chapter 2 provides a literature review on the channel restoration structures of interest. Chapter 3 contains the energy loss and backwater effect study to determine the effect of structure design and orientations for stream barbs, spurs, submerged vanes (and equivalent configurations), as well as large boulders. Chapter 4 contains the dye-trace study to determine the ability of structure design and orientation to provide additional vertical mass transport in open channel flow for stream barbs, submerged vanes, and large boulders. Chapter 5 presents the conclusions of the research conducted in both the energy loss and vertical mass transport studies for channel restoration structures. This chapter also describes the engineering significance in the ability to compare various channel restoration structures and provides recommendations for future research. The appendices contain multiple images of the study experiment design parameters, as well as experimental data.

## CHAPTER 2.

### CHANNEL RESTORATION STRUCTURES

The channel restoration structures of interest include stream barbs spurs, submerged vanes, and large boulders. Major design handbooks and manuals include: *River Training and Sediment Management with Submerged Vanes*, ASCE (Odgaard 2009), *Stream Restoration Design*, NRCS NEH-654 (2007), *Stream Corridor Restoration*, NRCS (2001), *River Training Structure and Secondary Channel Modification*, UMRS-EMP (2012), *Guide to Placement of Wood, Boulders and Gravel for Habitat Restoration*, Oregon Department of Forestry/Fish & Wildlife (1995), *Design of Spur-Type Streambank Stabilization Structures*, Department of Transportation (1985). A summary on channel restoration technologies and project analysis has been performed by Robert Radspinner (2009). The U.S. Army Corp of Engineers has conducted an extensive and critical review in *Summary of Research on the Effects of River Training Structures on Flood Levels* (2014). The following is a general, non-inclusive review on commonly used structures of interest; stream barbs and spurs, vanes, and large boulders.

#### 2.1 Stream Barbs

Channel restoration projects often include the use of stream barbs. Along stream banks, barbs are arranged to redirect flow resulting in a reduction of shear stress and turbulence in order to protect stream banks against erosion while allowing for sediment deposition and habitat for aquatic and microbial life. Stream barbs, also known as rock vanes or rock dikes, are commonly used bank stabilization and flow control structures by the U.S. Army Corps of Engineers. Stream barbs behave like dikes, groynes, or spurs, due to bank anchoring with structure protrusion into the flow path to reduce streamwise velocity and shear stress. Differences in design from other bank aligned structures is the unique block based trapezoidal shape designed with side slopes of approximately 45°. The slope allows for flow overtopping and redirection toward stream center with minimal turbulence or scouring compared to structures perpendicular to stream flow (USDA, 2013). Design guidelines suggest a length to width,  $L/W$ , ratio of 3, with the structure

protruding out into the flow one-third or less of the channel width,  $w$ . The structure is typically designed so that the height of the structure at the bank is equal to water depth,  $d$ , (Figure 1).

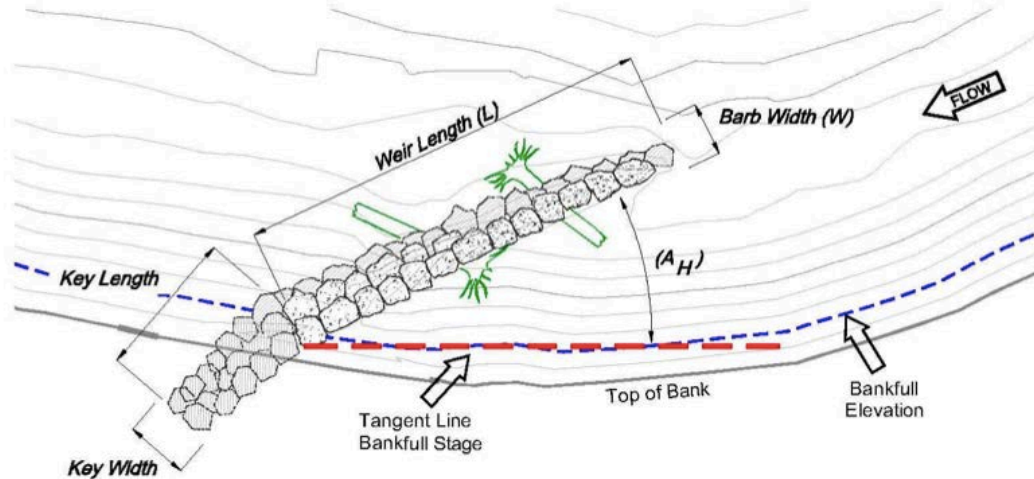


Figure 1. USDA Design of a Stream Barb, 2013.

Stream barbs have been shown to improve stream ecology through habitat diversity provided by the protective nature of the structure. However excessive flooding or flow velocities have been shown to result in high failure rate or low life span of such technologies due to inadequate design and construction of such technologies. Scour and sediment dynamics induced by stream barbs have been most recently studied by Fox et al. (2005) and Jamieson et al. (2013), with a two-dimensional (2D) computational model developed by Hossain et al (2013). Similar shaped structures without the use of rock include thin vertical structures known as spurs that also provide significant bank stabilization.

## 2.2 Submerged Vanes

Alternatively, shear stresses and vertical mass transport can be managed, enhanced or reduced as necessary by using submerged vanes, or “Iowa Vanes”, placed so as to generate stream-wise vortices in desired locations of the channel (Odgaard, 2009). Submerged vanes appropriately engineered create a secondary current or spiral motion in the flow downstream, which alters the shear velocity distribution and enhances vertical

mass transport with little additional turbulence and energy loss. Along stream banks, this spiral prevent bed and bank shear stresses greatly reducing soil erosion. Submerged vanes are thin vertical flow training structures most commonly aligned in an array angled against the direction of flow,  $\alpha$ . Submergence ratio,  $d/H$ , where  $d$  is the water depth and  $H$  is the height of the structure is typically 2 to 5, however bank stabilization can be achieved in water depths eight times the height of the vane system. Length to height ratio,  $L/H$ , is typically 2 to 3.

Submerged vane at a small angle of attack induce a horizontal circulation in the flow downstream (Figure 2, top). The circulation arises because the vertical pressure gradients on the two surfaces of the vane cause the fluid flowing along the high-pressure (upstream) side to acquire an upward velocity component, whereas on the low-pressure (downstream) side there is a downward velocity component. The resulting vortices or

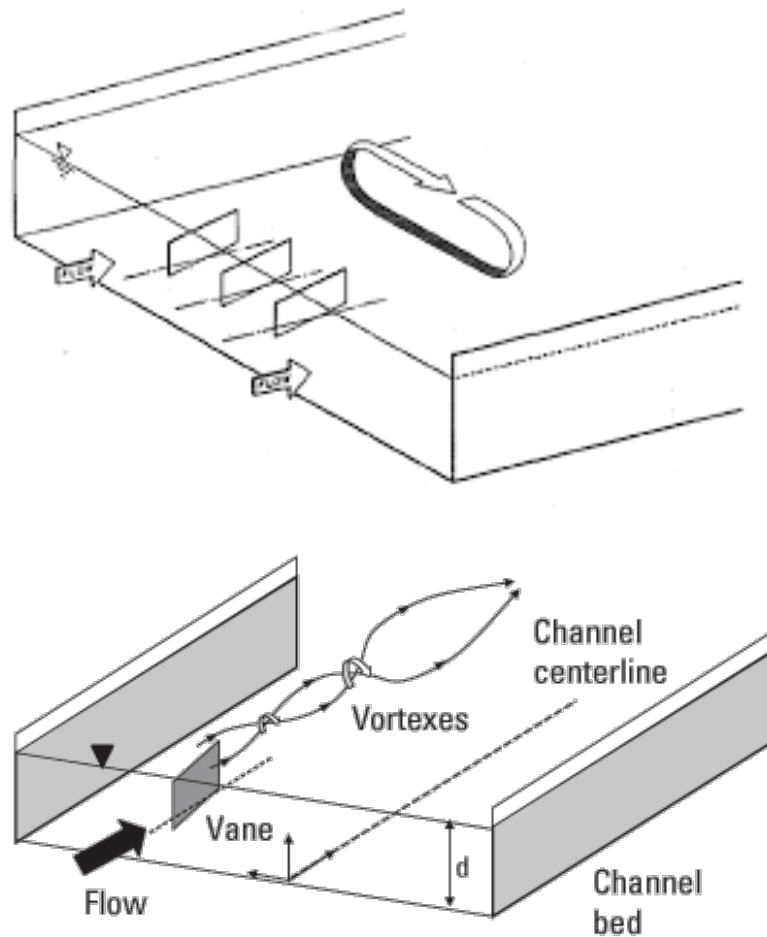
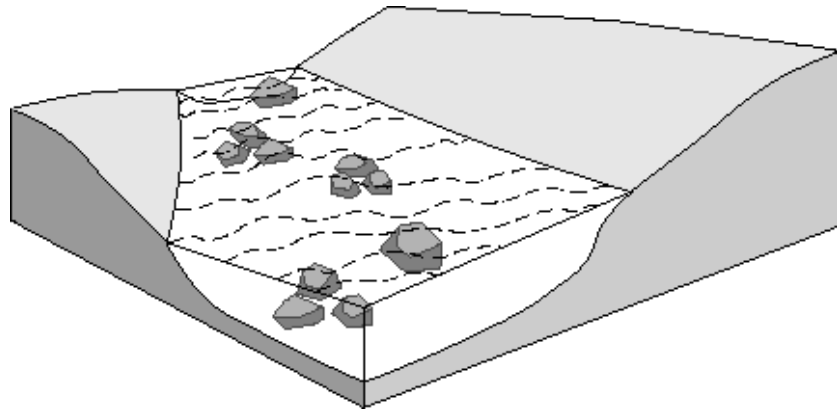


Figure 2. Single submerged vane induced vortices (Top) and array of vanes inducing counterclockwise mixing, Odgaard, 2009.

vortex sheet at the trailing edge of the vane roll up to form a large vortex springing from a position near the top of the vane. This vortex is carried with the flow downstream, where it gives rise to a secondary or helical motion of the flow and associated changes in bed shear stress. When aligned in an array, in Figure 2 (Bottom), a strong mixing or clockwise circular motion is produced (Odgaard, 2009). These changes can be calculated (Odgaard and Wang, 1991; Wang and Odgaard, 1993).

### **2.3 Boulders**

Stream restoration is frequently managed using rocks and large boulders strategically placed to create a level of turbulence within the stream segment while providing additional ecosystem habitat (Hamuy-Blanco, 2014). The natural stone material is economical and deliver aesthetic appeal in channel restoration efforts. Several channel restoration designs utilizing boulders has been presented by the NRCS, with a cluster boulder example given in Figure 3.



*Figure 3. Boulder cluster design by NRCS, NEH, 1998.*

Structures placed in the line of flow produce vertical mass transport by the process of turbulent dispersion, enhanced by the wake turbulence and flow separation behind the structure. The wake turbulence also modifies the shear stress distribution, as scouring and sediment deposition can be controlled. Scour holes and increased turbulence provide beneficial aquatic habitat to channels with little geomorphological diversity. Greatest benefit for the introduction of large boulders has been in streams with average

flows greater than 2 ft/s, and in wide shallows streams with gravel and rubble beds. Turbulence generation causing excessive erosive forces limit the capabilities for streams of low slope or degraded sloped streams, and to those of sand or fine beds (Bernard, 1998). Due to the structure design, little stream bank stabilization is produced, unless specifically designed to intercept high velocity flow around banks and bends from causing stream instability.

## **CHAPTER 3.**

### **ENERGY LOSS AND BACKWATER EFFECT STUDY**

A comparison is made of the flow-energy loss associated with channel restoration structures utilizing stream barbs, spurs, submerged vanes and large boulders. The comparison is limited to subcritical flows and structures that are submerged and/or angled upstream into the oncoming flow at relatively small angles of attack. The energy loss is calculated from standard, high-Reynolds-number-drag force relations. The drag force for submerged vanes that are located away from banks is obtained from analogy with airfoil theory. The relationships are validated in laboratory tests. The study shows that a system of submerged vanes can be designed to provide the same erosion protection of a given stream bank as can a system of upstream-angled spurs or stream barbs and can accomplish the task at comparable, and sometimes less, energy expenditure. When placed away from the bank submerged vanes are more efficient (in terms of energy expenditure) than spurs and boulders in channel restoration efforts. Findings comparing stream barbs and spur structures were presented at the *World Environmental and Water Resources Congress* (Odgaard, 2016), while research comparing submerged vanes and blocks were presented at the *River Flow Conference* (Odgaard, 2016).

#### **3.1 Introduction**

Evaluation of common channel restoration structures was performed utilizing a fixed bed rectangular flume. The channel restoration structures of interest in this study include stream barbs and similarly designed spurs, submerged vanes, and large boulders. The submerged vanes are located and oriented such that near-bank bed load is continually intercepted and deflected toward the bank, partially filling the scour holes that would tend to form at the tip of the spurs. Moreover, the vanes also create a horizontal circulation of the flow that helps maintain vertical mass flux in the area close to the bank. Large boulders have been common in restoration efforts, due to the natural stone material and improved aesthetics, with the goal to induce momentum reduction through wake turbulence and turbulent dispersion (Hamuy-Blanco, 2014).



Spur dike systems are comparable to stream barbs, they are bank anchored, however typically a thick vertical metal structure angled out into the channel, either perpendicularly or angled with the direction of flow. Spurs investigated in this study include design similar to stream barbs, as well as those integrated with the design of vanes. Part of the energy loss around the spurs is from the turbulence created at the tip of the spurs. Separation eddies and vortices at the tip increase turbulent intensity and bed shear stress in the flow around the tip. In case of a movable bed, the bed typically scours at and immediately downstream from the tip. From an ecological point of view, the scour is considered beneficial. However, at high velocities the scour holes often become excessive compromising the integrity of the spurs. In addition, with the spur-only solution the lower velocities closer to the bank may reduce vertical mass flux right at the bank resulting in potential ecological or water quality problems. A solution that may obviate these concerns is the vane-spur combination (Figure A-10).

### **3.2 Energy Loss Theory**

Flow of water within a river or stream is subjected to frictional forces (drag) from the stream bed, banks or sides of the channel, and from vegetation or structures placed within the field of flow. Large structures such as bridge columns, large boulders and channel restoration structures can exert significant drag on the flow resulting in energy loss. Reduction in the momentum of flow causes decrease in velocity, resulting in a rise of water level upstream, also known as backwater effect, BWE. The capacity for channel restoration structures to induce backwater and reduce the ability to transmit high flow conditions have been thought to be partial cause for the observed increase in flooding (Azinfar, 2011). Significant research in hydraulic engineering is being performed on physical and computer based models to better understand the relationship between structure design and energy loss to be able to predict impact of stream hydrodynamics on surrounding areas.

Energy loss can be expressed through the energy approach or momentum approach. Momentum is mathematically defined for open channel flow with use of the Reynolds Averaged Navier – Stokes Equations (RANS). Assuming incompressible flow,

non-convective, steady state, constant pressure head, with negligible Coriolis effect the change of momentum per unit volume is a function of surface forces including viscous and Reynolds stresses, as in Eq. 3.1, for homogeneity of flow in the x and y direction.

$$\frac{1}{\bar{p}} \frac{\partial \bar{p}}{\partial x} = \frac{1}{\bar{p}} \frac{\partial}{\partial x} [\tau_{xz}^{viscous} - \tau_{xz}^{Reynolds}] \quad \text{Eq. (3.1)}$$

The momentum approach executed on an upstream and downstream segment of the open channel is often preferred. For one-dimensional flow the linear momentum equation results in Eq. 3.2, as similar to the work by H. Azinfar and J. A. Kells on backwater analysis of spur dikes (2008; 2010; 2015):

$$F_1 - F_2 - F_D - F_f + F_w = \rho Q(\beta_2 u_2 - \beta_1 u_1) \quad \text{Eq. (3.2)}$$

Where  $F_1$  = force due to the upstream hydrostatic pressure,  $F_2$  = force due to the downstream hydrostatic pressure distribution,  $F_D$  = drag force due to the presence of submerged structures,  $F_f$  = frictional force due to surface boundary and shear stress between upstream and downstream segments,  $F_w$  = gravitational component due to the weight of the fluid. In the case of steady uniform flow, the frictional force is equal to the gravitational force, ( $F_f \cong F_w$ ). The momentum correction factors  $\beta$  is often assumed to be unity for open channel flow (Azinfar, 2008). The impact of a submerged structure field results in highly three-dimensional flow, nonhomogeneous in the x and y direction. For simplicity the channel's energy slope is estimated using the momentum equation on a control volume between two sections of the channel, one section just upstream of the structure system and the other just downstream from the system. By neglecting the structures' effect on the momentum fluxes in and out of the control volume (i.e., by assuming they are practically equal in magnitude), the momentum equation becomes a simple force balance:

$$F_f + F_D = \rho g b l d (S_o + S_f) \quad \text{Eq. (3.3)}$$

Where  $b$  = width of channel,  $d$  = design uniform-flow depth,  $l$  = distance between upstream and downstream sections,  $S_o$  = slope of channel, and  $S_f$  = induced increase in

energy slope, or  $\Delta S$ . The drag force exerted on the flow by an object is related to its drag coefficient,  $C_D$ , upstream projected area of the structure,  $A_p$ , and mean velocity,  $u$ , and is expressed by:

$$F_D = C_D A_p \rho u^2 / 2 \quad \text{Eq. (3.4)}$$

### Stream Barb

The drag coefficient for the stream barb,  $C_{D,SB}$ , with a projected area  $A_p$  facing streamwise flow. When constructed with perfect equilateral triangular section, the stream barb drag coefficient would be  $c_{D_s} \approx 1.0$ . Stream barbs, including the model versions used in the laboratory, do not have a well-defined  $90^\circ$  top edge, which is a defining feature of the ‘equilateral triangular section.’ The rocks make the edge somewhat rounded. Consequently, the flow passing over the top creates less separation than does a defined  $90^\circ$  top edge, and a somewhat lower drag coefficient is expected. It is reasonable to select a value in between Blevins’ ‘equilateral triangle section’ value of 1.0 and his ‘semicircle section’ value of 0.8. A value of 0.9 is adopted. Blevins’ assessment of the error on any of the values is  $\pm 20\%$ . For sloping stream barbs,  $A_p = \frac{1}{2}HL\sin\alpha$ . The induced change in slope or change in water depth over the length of the system of  $N$  equal-sized, equal-spaced stream barbs can be determined using:

$$\Delta S_{SB} = \frac{\Delta d}{\ell} = \frac{1}{2} C_{D,SB} \frac{NA_p}{b\ell} \frac{u^2}{gd} \quad \text{Eq. (3.5)}$$

### Spur Dike

The spur-drag coefficient is the order of 1.0 to 1.4, depending on the cross-sectional shape of the spur (Blevins 2003). Structures with a ‘fence section’ the value is about 1.4; for a ‘square section’ (not tested) the value is about 1.2; and for an ‘equilateral triangle section’ the value is about 1.0. For the rectangular flat-panel rectangular spur used in the spur-vane system,  $A_p = HL\sin\alpha$ , and sloping flat-panel triangular spur (similar to stream barb)  $A_p = \frac{1}{2}HL\sin\alpha$ , with  $c_{D_s} \approx 1.4$ . Vertical spur theoretical energy loss can be calculated using Eq. 3.5 while the increase in energy slope from the vane-spur combination is calculated with the combination of Eqs. (3.5) and (3.8).

## Metal Vane

Momentum theory analysis to determine the energy loss from submerged vanes has been developed from an airfoil analogy (Odgaard, 2009). By assuming ideal flow around the vane, the horizontal circulation is calculated by relating it to the horizontal lift force,  $F_L$ , which the vane exerts on the flow. This lift force has the same magnitude as the force that the flow exerts on the vane. Which, according to the Kutta-Joukowski theorem (Sabersky and Acosta 1964), is proportional to the vertical circulation around the vane associated with the shift of the rear stagnation point to the trailing edge of the vane. This vertical circulation, in turn, is equal to the horizontal circulation (Helmholz's second theorem). The drag force associated with a system of  $N$  independent submerged vanes is:

$$F_{D,MV} = N \frac{1}{2} c_{D,MV} \rho L H u^2 \quad \text{Eq. (3.6)}$$

Where  $C_{D,MV}$  = vane-drag coefficient,  $\rho$  = fluid density, and  $u$  = fluid velocity. By assuming distribution of vertical circulation around the vane is elliptical (maximum at the bed and zero at the top of the vane) the vane-drag coefficient is:

$$c_{D,MV} = \frac{L}{e 2\pi H} C_L^2 \quad \text{Eq. (3.7)}$$

The lift coefficient is  $C_L = 2\pi\alpha/(1+L/H)$  (Odgaard and Spoljaric 1989, Odgaard and Mosconi 1987). For angles of attack larger than  $7^\circ$ , flow separates from part of the low pressure or suction side of the vane before reaching the trailing edge, and the lift distribution is not elliptic. The deviation from an elliptic distribution is often accounted for in tip vortices and results in Oswald's efficiency number,  $e$  (Anderson, 2008). For flat-plate rectangular wing shapes,  $e$  is typically about 0.7 due to tip vortices. The change of slope induced by a system of  $N$  independent vanes produces a backwater  $\Delta d$  over a given length,  $\iota$  of the system:

$$\Delta S_{MV} = \frac{\Delta d}{\ell} = \frac{\pi\alpha^2}{e} \frac{L/H}{(1+L/H)^2} \frac{NHL}{b\ell} \frac{u^2}{gd} \quad \text{Eq. (3.8)}$$

## Frontal Projections and Blocks

To compare the momentum and theoretical energy loss relationships produced by vanes, the investigation on similarly designed objects of projected area,  $A_p$  was performed. Where  $A_p = HL\sin\alpha$ , and  $\alpha$  is the angle of the vane or vane equivalent. Frontal projections known in this thesis consist of thin plate perpendicular to flow, as well as full blocks or rectangular blocks that are constructed with equivalent projected area and length. The energy loss caused by a field of rectangular, equal-sized, equal-spaced frontal projections or blocks with no mutual interaction is:

$$\Delta S_{FP,BI} = \frac{\Delta d}{\ell} = \frac{1}{2} C_{D,PF,BI} \frac{NHL\alpha}{b\ell} \frac{u^2}{gd} \quad \text{Eq. (3.9)}$$

Structures are equal to the stream wise projected area as a function of the angle of the vanes, creating a protuberance or a fence section, with a  $C_{D,FP}$  value of 1.4 for frontal projections (Blevins, 2003). Full blocks are long rectangular solid object that induce heavy blockage compared to the nature of vanes and frontal projections. For a rectangular block of height  $H$  and length,  $L$ , the drag coefficient is a function of the  $L/H$  ratio, for increasing  $L/H$  from 1 to 3,  $C_{D,BI}$  decreased from 2.2 to 1.3, and for a value of  $L/H = 2$ ,  $C_{D,BI} = 1.6$  to 1.4, with 1.4 suggested (Blevins, 2003).

## Large Boulders

Large boulders were constructed in this experiment so that the circular shape would not introduce additional variability or turbulence in the analysis due to the irregularity in natural boulders. A system of  $N$  independent hemisphere boulders will induce a change of slope onto the channel as in Eq. 3.10:

$$\Delta S_B = \frac{\Delta d}{\ell} = \frac{1}{2} C_{D,B} \frac{NA_p}{b\ell} \frac{u^2}{gd} \quad \text{Eq. (3.10)}$$

The drag coefficient for a hemispherical protuberance structure,  $C_D$ , is 0.4 to 0.6 under low Reynold's flow conditions and 0.1 for flows with  $Re > 2 \times 10^5$  and upstream projected area,  $A_p = \pi L^2/8$  (Blevins, 2003).

### 3.3 Methods

Experiments were performed in a 54-foot long, 3-foot wide, glass-walled, rectangular tilting flume at IIHR Hydrosience and Engineering (Figure A-1). Appendix A Figure A-3 and A-4 display details of the experimental setup. The bottom of the flume was smooth metal sheeting, and equipped with an adjustable incline system for channel slope,  $S_0$ , of 0.00 to 15.00% with 0.01% degree of accuracy. The flume was constructed in six-foot sections, provided baseline for structure placement and measurements. Water was circulated through the flume using centrifugal pumps and flowrate was measured with calibrated orifice meter in the supply pipeline. Flow depth was controlled with a standard tailgate at Section 9.

Channel restoration structures tested for energy loss include stream barbs, spur, vanes and boulders. Submerged vanes were constructed according to Odgaard and ASCE standards, and stream bars were constructed according to NRCS design standards. Submerged vanes, spur, and stream barbs were made from 20-gage galvanized steel (0.0396-inches), while frontal projections and blocks were of wood, and boulders of concrete. Stream barbs were formed into typical tetrahedron shape and covered in a waterproof masonry glue pebble rock mixture to simulate in-stream rock-barb roughness (Figure A-6). Large boulders were constructed into hemispherical shapes to reduce variability within flow structures, to resemble NRCS boulder cluster design (Figure A-19).

In submerged vane, spur, block and boulder experiments height was  $H = 4$ -inches for a submergence ratio,  $d/H$ , of 2 and length was  $L = 8$  inches (Figures A-8, A-10, A-12, A-14 and A-18). Blocks and frontal projections structures utilized in the experiment consisted of the same shape and streamwise projected area (Figure A-15). Block structures were designed to directly compare to vanes, height,  $H$  of 4-inches and  $L = 8$ -inches, while frontal projections were constructed with a length,  $L$  of 0.25-inches and attached to the vane orientated at zero-degrees, for stability. Metal vane, block, and frontal projection systems were constructed so that each array consisted of 5 individual vanes spaced 6-inches apart and located within the center of the flume (Figure A-14). Stream barbs were constructed at submergence ratio 2 and 1 or  $H = 4$ -inches and  $2H = 8$ -

inches, at the highest point of the structure to be half the water depth or just at the water depth (Figure A-5). Spurs were tested to evaluate the effectiveness of the sloped sides of the stream barbs in redirection of flow at  $H = 4$ -inches only. Length of the stream barbs and spurs were 36 inches connected to the side of the flume angled at  $27^\circ$  toward the direction of flow. Additional restoration structures were designed to incorporate the integration of vanes anchored to the stream bank or flume wall. These included a three metal vane array system (Figure A-10), where the outmost vane was attached to the flume wall. The other system of interest for observation included a two metal vane array system located 6-inches from the flume wall combined with a small ramp to provide additional forcing for horizontal vortices and redirection of flow from the bank or flume wall (Figure A-12).

### **3.4 Backwater Effect (BWE) Experimental Procedure**

Uniform flow was established, without submerged structures in the flume, by successive tests involving small adjustments of channel slope, discharge, and tailgate setting. Target values were a velocity,  $u$ , of 0.8 ft/s and a flow depth,  $d$ , of eight-inches along the entire length of the flume. Steady state at such values were achieved with a channel slope,  $S_o$ , of approximately  $2.0 \times 10^{-4}$  or 0.02%. Metal clips were attached to the flume floor to allow for in-experimental structure removal and/or orientation change. Headloss induced by the metal clips were minimal and within the level of accuracy. Steady state flow conditions were allowed to develop over a period of 2 to 3 hours for each experiment until discharge was maintained at  $1.6 \text{ ft}^3/\text{s} \pm 0.015 \text{ ft}^3/\text{s}$ . Submerged structure orientation or model changes during flume experiments were allowed to reach steady state flow conditions within 15 to 30 minutes. Attention was taken that the depth at the most downstream measuring Section 8 remained at 8-inches ( $\pm 0.10$ -inches due to tailgate setting limitations). Water depth elevations were measured with an accuracy  $\frac{1}{2}$  a sixteenths of an inch or  $\pm 0.031$ -inches.

The submerged structures were installed at Section 2 through 7, as indicated in Figure 17. The most downstream array of restoration structures was located 12-feet upstream from the tailgate (Section 9). The arrays were spaced 3 feet apart, so that

shielding was avoided. There were eleven arrays for a field system, for 55 total structures for the vanes, frontal projections or blocks (5 structures per array), and 11 total structures for the stream barbs and spurs (one structure per array). Additional experiments were performed with a field of 6 arrays placed at twice the distance of separation for vanes and boulders. Summary of backwater effect study structure and orientation designs under investigation are listed in Table 1.

Table 1. Backwater effect and energy loss on channel restoration structures.

		<i>SUBMERGENCE RATIO</i>	<i>LENGTH, INCHES</i>	<i>HEIGHT, INCHES</i>	<i>ANGLE</i>	<i>NUMBER IN FIELD</i>	<i>NUMBER PER ARRAY</i>
<b>VANES:</b>	VANE	2	8	4	0/5/10/15/ 20/25°	6, 11	5
	PROJECTIONS	2	8	4	10/20°	11	5
	FULL BLOCKS	2	8	4	10/20/25°	11	5
	WALL VANE	2	8	4	20°	11	3
	VANE- RAMP SYSTEM	2	8	4	0/5/10/15/ 20/25°	11	2
<b>STEAM BARB:</b>	ROCK BARB	1, 2	36	8, 4	~27°	11	1
	SPUR MODEL	2	36	4	~27°	11	1
<b>BOULDER:</b>	HALF SPHERE	2	8	4	-	6, 11	2

The change in water surface elevations by the system of restoration structures was measured along Sections 1-8, for stream barbs (Figure A-7), spurs (Figure A-9), vanes and equivalent blocks and frontal projections (Figure A-16), wall attached vane system (Figure A-11), vane ramp system (Figure A-13), and large hemispheres resembling boulders (Figure A-17). Measurements were collected and repeated over a period of time for a total of 4 to 10 data series per experiment. Target tail-water depth, slope, and flowrate were checked before each data collection. Flowrate fluctuations were recorded with lowest and highest readings observed for 1-minute for each data series in the experiment. Standard deviation in flow rate for each structure experiment was  $\pm 0.002$  to  $0.009 \text{ ft}^3/\text{s}$ , and change in water depth at each station of  $\pm 0.00$  to  $0.02$ -inches. Water depth measurements were observed on both sidewalls, and before and after structures for Sections 2, 3, 6, and 7 to determine if additional areas where of interest.

At least two separate experiments were conducted for each structure layout. Values were evaluated against theoretical relationships to determine observed drag



coefficients and efficient number. Submerged vanes were tested at orientations with angles,  $\alpha$ , 0 to 25 degrees with 5 degree increments, while 10 and 20 degrees was tested for the reduced field with 6 arrays. Blocks were tested at orientations with angles 10, 20 and 25 degrees, while frontal projections were tested at 10 and 20 degrees. Vane – ramp system was evaluated for vane orientations at 0 to 25 degrees with 5 degree increments, and vane – wall attached system was tested at 20 degrees, both at 11 array field. Stream barbs were tested at both heights for a submergence ratio or 1 or 2. Spurs and stream barbs were tested at their single design as noted above for an 11 array field placed with each array at a 3-foot spacing. Boulders were oriented so that two boulders per array, with boulders staggered along the width of the flume to reduce channelization of flow. Boulders were tested for a total of 11 and 6 arrays.

The change in water depth measurements were adjusted for measurement discrepancies in flow as indicated in clean flume flow conditions, and normalized with uniform-flow depth  $d$  of 8-inches at Section 9 to eliminate tailgate height limitations. Due to restrictions in flume length, data was then again normalized to obtain a depth  $d = 8$ -inches at Section 7, location of the last set of structures within the field to eliminate inconsistencies due to backwater by the presence of the tailgate in high headloss situations, resulting in  $N'$ . Values were evaluated against theoretical relationships to determine observed drag coefficients and efficient number.

### **3.5 Results**

The field of channel restoration structures ability to induce energy loss and backwater effect was investigated for common channel restoration structures, as well as some additional structures of interest and found in Tables B-1 to B-5 in Appendix B. Standard deviation in change in height at each section ranged from 0.00 to 0.02-inches for all structures. Change in water depth at Sections 1 to 7 (0 to 36 feet) for structures are plotted in Figure 4 to 8, including standard deviation for all data measurements in each trial. Theoretical energy loss relationships for the channel restoration structures are compared to experimental measurements in Table 2 using Equations 3.5, 3.8, 3.9 and 3.10. Typical drag coefficients, or efficiency number for submerged vanes, result in an

acceptable  $\pm 20$  to 50% difference due to flow characteristics. It was found for several structures, design orientation or spacing resulted in large discrepancies from published values. Experimentally determined drag coefficients,  $C_D$ , and efficiency number,  $e$ , were determined for stream barb, spurs, vanes, blocks and boulder systems.

Table 2. Backwater effect measurements compared to theoretical values.

Design	$N'$	$\Delta d$ , Estimated	$\Delta d$ , Exp.	$C_D$	
				Estimated	Exp.
8-in Stream Barb	8-in 10	0.25	0.21	0.9	0.75
4-in Stream Barb	4-in 10	0.13	0.07	0.9	0.50
4-in Spur	4-in 10	0.20	0.12	1.4	0.85
3 Vane – Wall System	4-in 30	0.13	0.13	0.31 1,4	0.31, 1.4
2 Vane – Ramp System	4-in 20	0.06	0.10	0.31	0.45
Full Block	10° 50	0.16	0.18	1.4	1.55
	20° 50	0.33	0.40	1.4	1.75
	25° 50	0.40	0.70	1.4	2.42
Vane	5° 50	0.01	0.02	0.02	0.04
	10° 50	0.04	0.06	0.08	0.11
	10° 25	0.02	0.04	0.08	0.13
	20° 50	0.16	0.16	0.31	0.31
	20° 25	0.08	0.11	0.31	0.43
Boulder	25° 50	0.25	0.34	0.48	0.65
	4-in 20	0.04	0.21	0.6	3.1
	4-in 10	0.02	0.06	0.6	1.9

Change in depth observed for an 11 vanes array field is shown in Figure 4. Submerged vanes from 0 to 25-degrees displayed change in water depth of 0.02 to 0.34-inches. Vanes angled at 5-degrees display little to no backwater effect (0.02 inches) to those angled at 0-degrees (0.04-inch). Sharp increase in water depth change is noticed at orientations greater than 10 degrees with increased backwater at 25 degrees. Small dissimilarities in theoretical change in water depth were observed for 10 and 25 degrees, while efficiency number of 0.7 was accurate for vanes at 20 degrees. The calibration factor for 10, 20 and 25-degrees at these flow and submergence conditions would most closely be expressed by efficiency number,  $e$ , of 0.50, 0.70, and 0.52 respectively.

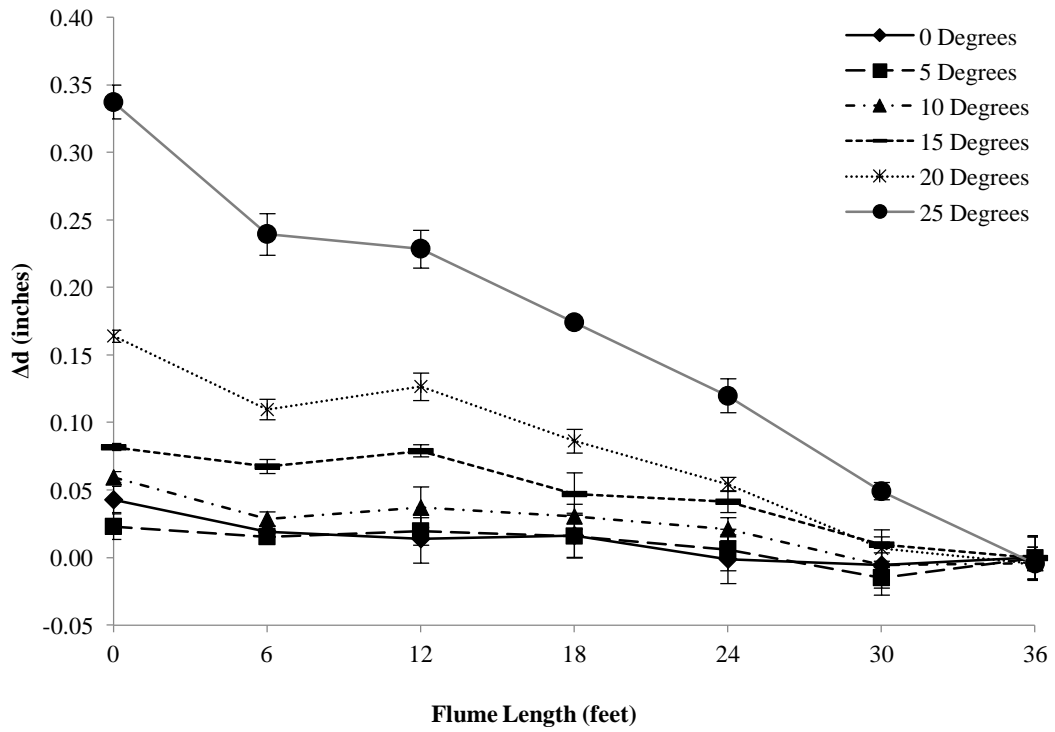


Figure 4. Backwater effect measurements by different vane orientations, at 0 to 25 degrees in 5 degree increments, with 5 vanes array field of 11.

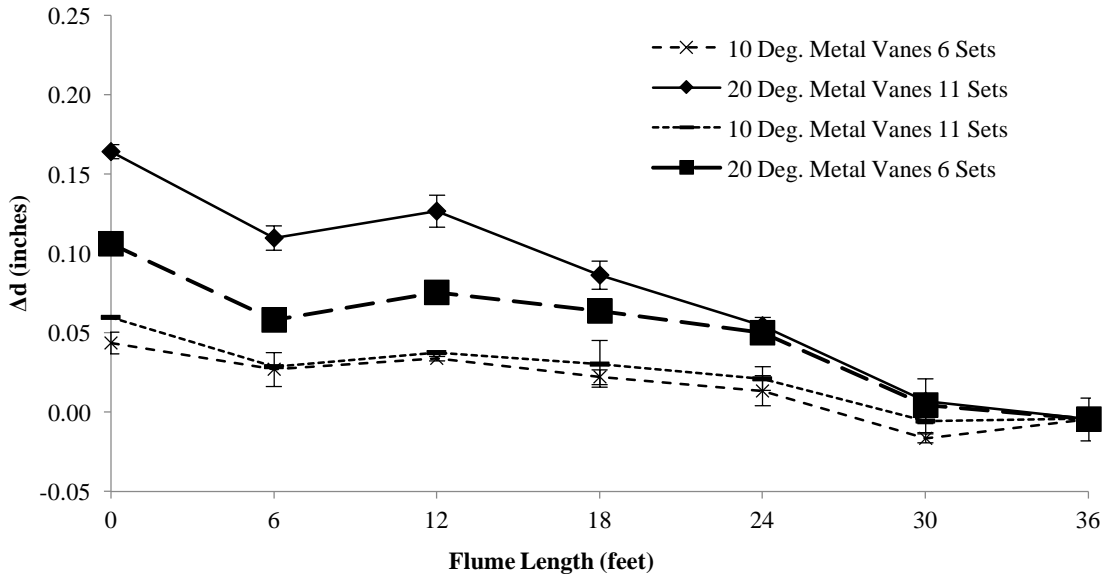


Figure 5. Backwater effect measurements by different number of vane arrays.

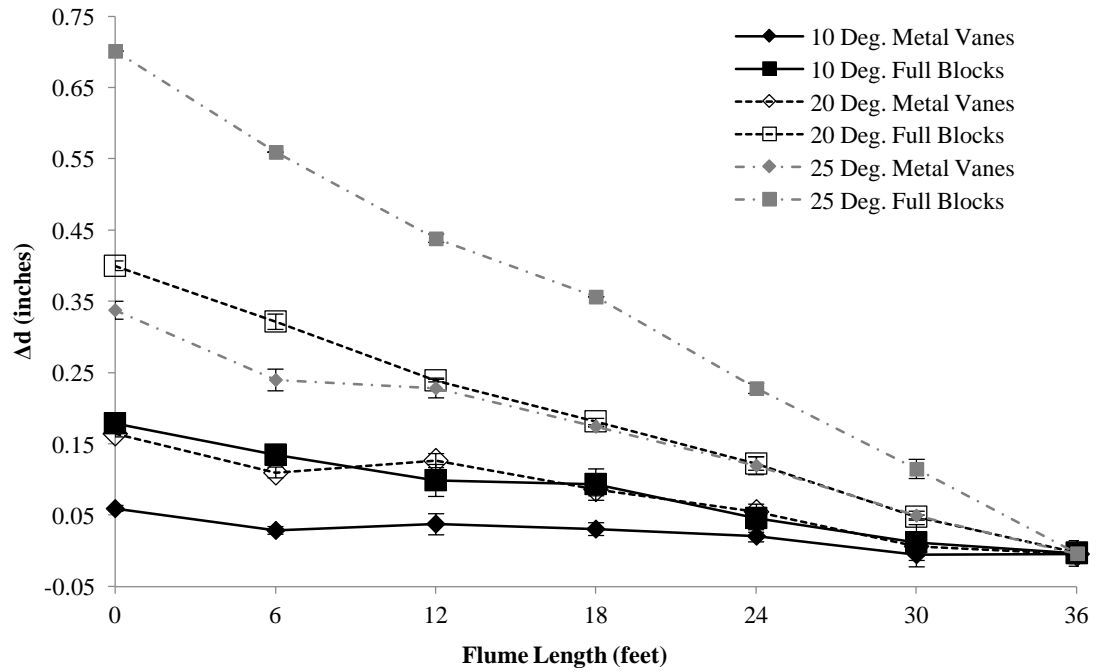


Figure 6. Backwater effect by vane system compared to frontal projections and full blocks, at 10, 20 and 25 degrees.

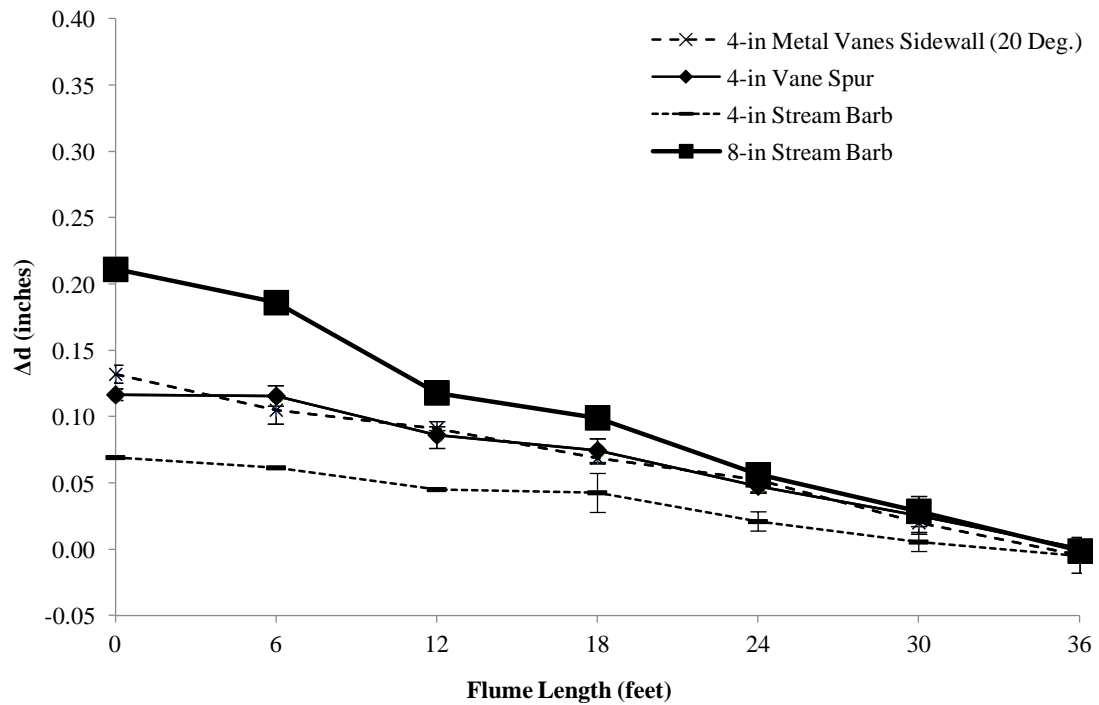


Figure 7. Backwater effect by stream barb, spur and vane attached systems.

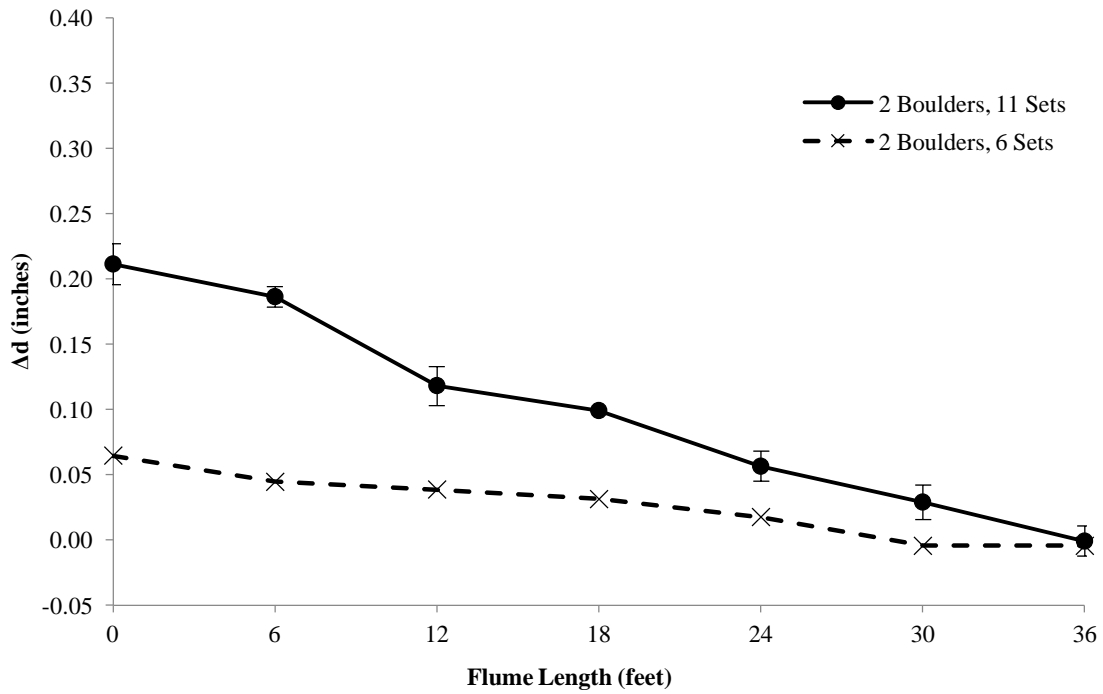


Figure 8. Backwater effect by boulder system.

The effect of spacing on energy loss and backwater effect for vanes angled at orientations of 10 and 20 degrees is shown in Figure 5. Increased number of 10-degree vane arrays in a given field has little effect on backwater or momentum loss of channel flow as compared to 20-degrees. When the spacing of the system was doubled from 3-feet to 6-feet for a total of 6 array field of vanes the efficiency number,  $e$ , were reduced to 0.40 and 0.50 for the system of 10 and 20 degree vanes.

Frontal projections and full blocks at equivalent streamwise area of the vanes produced significant backwater effect. Back water effect from submerged vanes compared to equivalent block system is displayed in Figure 6. Backwater effect from a block field at equivalent 10, 20 and 25 degrees was 0.18, 0.40 and 0.70-inches respectively. Frontal projections have been omitted from this section due to the obstruction of turbulence and energy dissipation presented by the 0-degree vanes used to provide structural integrity into the system. As expected in theory, the angular momentum generated by the vanes results in a lowered energy expenditure compared to full blocks. However, as the projected area increased blockage effect had greater impact on blocks of 20 and 25-degrees. Blockage effect at orientations greater than the

equivalent 20 degrees results in a theoretical underestimation, resulting in an updated calibrated experimental drag coefficient,  $C_{Bl}$ , of 1.55, 1.75, 2.42, for 10, 20 and 25-degree blocks.

Stream barbs and stream barb equivalents, such as spur and wall vane systems are shown in Figure 7. Vane – ramp system has not been included due to limited capacity for adequate bank protection and sediment transport as shown in sequential dye tests. Stream barb, vane – wall system, and spur (metal vane model) system display reduced backwater effect at a submergence ratio of 2 ( $H = 4$ -inches) of 0.07, 0.13, and 0.12-inches, respectively. Stream barbs at a submergence ratio of 1 ( $H = 8$ -inches) have a backwater effect of 0.21-inches, similar to a 20-25-degree vane system. The trapezoidal structure, however spatially intrusive in a channel deliver effective bank stabilization with reduced energy loss compared to the spur model of the same upstream projected area and design. Interestingly a three vane wall system, consisting of two independent vanes and one vane, or dike, was not shown to decrease energy loss. Drag coefficients used in theoretical backwater estimations for all stream barb and equivalent bank anchored structures shows low levels of dissimilarity from observed change in water depth. However small and large stream barbs measurements correspond to reduced drag coefficient,  $C_{D,SB}$ , of 0.50 and 0.75 compared to 0.9.

Boulder system consisting of two boulder array spaced in stagger alignment to the stream wise velocity were tested with 6 and 11 array field (Figure 8), with values of 0.06 and 0.21-inches. Energy loss from a boulder system are comparable to a system of large stream barbs or the 20 to 25-degree vane system. However, backwater experienced by the two boulder array system at both a 6 and 11 array field were 400 to 200 percent more than theoretically predicted resulting in an adjusted calibrated drag coefficient,  $C_{D,B}$ , of 3.1 and 1.9 respectively.

### **3.6 Summary**

The study shows that the energy expenditure of a system of submerged vanes placed at an angle of attack of 10-degrees with the flow is only about one third that of a corresponding system of equivalent blocks, and just slightly less than a system of stream

barbs of the same submergence. A system of 20-degree submerged vanes resulted in higher efficiency for vortex forcing with a drag coefficient of 0.43 for arrays spaced 9 times the length of the structure (6-feet) compared to 0.31 with arrays spread 4.5 times the length of the structure, and 0.11 and 0.13 for a system of 10-degree vanes for the respective spacing. Energy loss from vanes angled at or above 20-degrees produced backwater effect or slope of friction comparable to that large stream barbs and boulders.

## **CHAPTER 4.**

### **VERTICAL MASS TRANSPORT STUDY**

A comparison is made of the vertical mass transport associated with channel restoration structures utilizing stream barbs, submerged vanes, and large boulders of various designs and orientations, including single and multiple-array fields. The experiments conducted were restricted to subcritical flows and structures that are submerged at half the water depth for stream barbs, vanes and boulders, and at full depth for a large stream barb. Submergence ratios were increased from 2, to 2.5 to 3.5 in order to determine the effects of water depth on a submerged vane's ability to induce vertical mass transport. The study shows that a system of submerged vanes can be designed to provide effective mixing, even at increased submergence ratios. When placed away from the bank submerged vanes are more efficient in providing channel mixing compared to stream barbs and boulders. whereas turbulent boundary layer from boulders of similar design show reduced ability to provide complete mixing at similar submergence.

#### **4.1 Introduction**

Hydrodynamic transport in open channels is governed by advection, turbulent dispersion, and to a lesser degree molecular diffusion. Turbulent dispersion is greater in the longitudinal direction compared to the vertical or convective. Though if present, are important mechanism along with the formation of longitudinal vortices (Ji, 2008). Due to the highly three-dimensional nature of open channel flow, vertical and longitudinal dispersion are considered independently. Wall or bank effects on turbulent dispersion are often too complex to parameterize, and as shown by Fischer (1979). In wide channels transverse mixing is still strongly affected by wall effects (Fischer 1979). The cross sectional area, slope, unsteadiness in flow, and the meandering nature produce turbulent kinetic energy and complicated flow and mixing dynamics.

Turbulence in shallow waters such as rivers is produced by chaotic and random velocity fluctuations due to velocity shear, waves, and flow separation around obstacles,



and at points of system inflow and outflow (Ji, 2008). Vegetation, aquatic animals, as well as subsurface and streambed microorganisms have also been found to induce turbulent mixing in rivers (Higashino, 2011; Battin, 2003). Advection-diffusion transport is of intense research interest regarding the many concerns over water quality, mass transfer and metabolic limiting factors. Analytic analysis tools include K- $\epsilon$  Theory, where the direct relationship between turbulent kinetic energy and dissipation is utilized in most Computational Fluid Dynamics (CFD) simulations. Evaluation of complex systems can be performed with Large Eddy Simulation (LES) and Direct Numerical Simulation (DNS) resulting in a large set of 3D flow characteristic parameterization that must be calibrated using physical models (Ji, 2008).

#### **4.2 Open Channel Mixing Theory**

Simplified empirical mixing relationships for open channel flow have been proposed by Fischer (1979) and are widely used (Socolofsky, 2005). Proposed equation have been modified over the past decade (Jirka, 2004; Dekota, 2009; Belayneh, 2012; Chau, 2000). Employing Elder's analysis and "Reynolds Analogy", with assumed logarithmic law relationship of flow velocity profile, the degree of turbulence within a steady straight rectangular channel can be parameterized by the bed shear or friction velocity,  $u_*$ , and the length scale of the largest turbulent eddy. The largest eddy in a channel is of the order of the water depth,  $d$ . The relationship reads the shear velocity in Eq. 4.1 is a function of the water depth and slope of the energy grade line (Fischer, 1979). Where slope of the energy grade line,  $S$ , is equal to the slope of the channel plus the induced slope ( $S_o + \Delta S$ ).

$$u_* = \sqrt{gdS} \quad \text{Eq. (4.1)}$$

The mixing coefficient of momentum can be related to the eddy diffusivity coefficient,  $\epsilon$ , for the vertical, horizontal or transverse directions as mathematically derived utilizing von Karman constant (Fischer, 1979):

$$\varepsilon = cdu_* \quad \text{Eq. (4.2)}$$

The vertical eddy diffusivity,  $\varepsilon_v$ , for non-rotating flow is expressed by Fischer for a rectangular straight channel,  $c_v$ , is typically 0.067, or 0.070 with  $\pm 50\%$  error (Rutherford, 1994). For comparisons transverse eddy diffusivity,  $\varepsilon_t$ , as investigation found that  $c_t$  corresponded to a values of 0.18 resulting in an error of  $\pm 30\%$  for various roughness experiments compared to 0.15 found by Fischer with  $\pm 50\%$  error (Chau, 2000).

Distance of complete mixing length,  $L_x$ , for centerline surface discharge of a dye plume to reach the side banks, also known as complete transvers mixing in Eq. 4.3 or to reach the bottom of the channel bed, known as complete vertical mixing or vertical mass transport in Eq. 4.4 (Fischer, 1979):

$$L_x = 0.1uw^2/\varepsilon_t \quad \text{Eq. (4.3)}$$

$$L_x = 0.4ud^2/\varepsilon_v \quad \text{Eq. (4.4)}$$

The role in advection diffusion may be significant in channels and streams, particularly those that include submerged structures where wave and tip vortices are induced into the flow. Using Fickian diffusion assumptions, Fischer describes the effects of advection on the rate of vertical mass transport provide additional re-aeration capacity generally attributed to molecular diffusion. The total rate of mass transport,  $q$ , in a three-dimensional flowing river or stream is:

$$q = u_z C (\text{advective flux}) + \left[ -\frac{D\partial C}{\partial x} \right] (\text{diffusive flux}) \quad \text{Eq. (4.5)}$$

Where  $C$  is mass concentration of the diffusive solute, and  $D$  is the diffusion coefficient, or molecular diffusivity with dimensions of (length)<sup>2</sup>/time. The average vertical velocity component,  $u_z$ , of a stream results from the fluctuating eddy velocity, or turbulence within a flowing water body. Generally, average vertical velocity component of flow is a small fraction of the streamwise velocity depending on the bed roughness and can be estimated from  $L_x$  in Eq. 4.6:

$$u_z = \frac{d}{L_x/u} \quad \text{Eq. (4.6)}$$

For typical channels length of complete mixing,  $L_x$ , estimated based on a factor of the water depth,  $d$ , is typically 12 to 50 (Jirka, 2005; Fischer, 1979).

### **4.3 Method**

Preliminary dye trace analysis was performed for each structure and orientation tested to observe flow dynamics and mixing characteristics. Dye tracer injection at streambed (flume bottom) and water surface, both at different locations relative to the structure and recorded using a typical photographic device. General nature of each structure and ability to provide vertical mass transfer was assessed. Due to the strong aerating capacity of the water fall at the end of the flume, as well as the deterioration of water quality from the piping system, investigation techniques to determine re-aeration rate were limited. The ability for structures to induce mixing and vertical mass transport was analyzed. Comparing different structure design and orientation to the length for complete mixing in the vertical direction, the additional average vertical velocity can be determined over clean channel flow or flume conditions.

### **4.4 Vertical Mass Transport (VMT) Experimental Procedure**

The rate of vertical mass transport was determined from a centerline injection of a specified quantity of neutrally buoyant dye. Injection was controlled by use of an acrylic burette with a polytetrafluorethylene (PTFE) plastic stopcock plunger to regulate flow at a given time interval. The burette was connected to a needle placed approximately 0.25-inches above the water level to allow the formation of a large dye droplet that would be released onto the water surface (Figure A-3). Each dye injection was observed for vertical and transverse motion. The length required for complete vertical mixing,  $L_v$ , as well as the location of streambed interaction or contact were recorded. Centerline injection was performed, as well at a location 6-inches away from the centerline. If the structures

displayed asymmetry, surface injection was conducted to both the left and right of centerline, and up to 12 inches as needed to determine impact of structure on vertical mixing. Each injection location was repeated at least 50 times. If molecular or turbulent dispersion occurred, no data was collected and the occurrence of ‘dispersion’ was noted, indicating no VMT was provided.

Structures tested for VMT included vanes, stream barbs, and boulders (Figure A-20 and A-21). A single stream barb of both heights was investigated. Submerged vanes and boulders were extensively investigated to determine the full impact of system design layout and orientation. A single array of the 1, 3 and 5 vanes at 10 and 20 degrees were tested. The impact of a second array in the system was also investigated for the vanes system angled at 20-degrees. Two single array systems were tested, as well as a 5 vane array followed by a 1, 3 and 5 vane array. A single marble covered or rock vane was tested at 20 degrees to simulate a more natural and less intrusive structure (Figure A-20). Boulders were investigated at different orientations including a single boulder, two boulders spaced 12-inches apart and 33-inches apart, a cluster of 4 boulders, a spaced cluster of 4 boulders each spaced 12-inches, and a system of two sets of two boulders angled at 45 degrees (Figure A-22). The influence of submergence ratio on the ability for vanes to facilitate VMT were of interest, two individual tests were performed on a single 5-set vane array angled at 20 degrees for submergence ratios: 2 ( $H = 8$ -inches), 2.5 ( $H = 10$ -inches) and 3 ( $H = 12$ -inches).

Table 3. Vertical mass transport and mixing study with channel restoration structures.

		SUBMERGENCE RATIO	LENGTH, INCHES	HEIGHT, INCHES	ANGLE	NUMBER IN FIELD	NUMBER PER ARRAY
<b>VANES:</b>	METAL VANE	2, 2.5, 3.5	8	4	10/20°	1, 2	1, 3, 5
<b>BARB:</b>	STREAM BARB	1, 2	36	8, 4	~27°	1	1
<b>BOULDER:</b>	HALF SPHERE	2	8	4	-	1, 2, 4	1, 2

The study provides a quantitative comparison in the ability for restoration structures to provide complete vertical mixing by the determination of  $L_x$  or vertical mass transport. Summary of VMT structure design and orientation can be found in Table 3. All experiments were normalized over clean flume observations. Experimental

observations include occurrence of complete vertical mixing or VMT, length of VMT,  $L_x$ , and transverse location of VMT.

#### **4.5 Results**

Preliminary dye tests were performed on all structures used in the backwater effect study, to determine optimal design and orientations for maximum vertical mass transport induced by the channel restoration structures. Extensive dye tracer experiments were conducted on stream barbs, vanes and boulders at various alignments. Figure 9 shows clockwise vortices from a 5 vane array with blue dye injected right above the channel bed and red dye injected on the water surface.

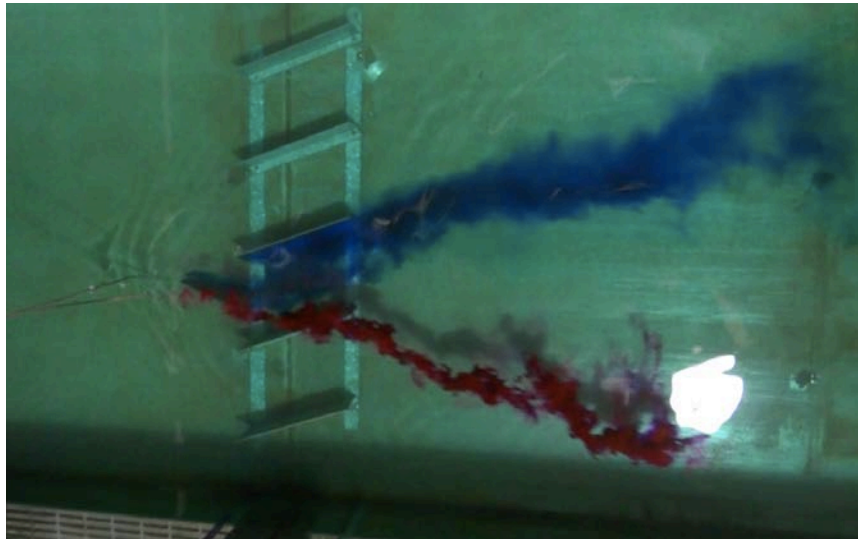


*Figure 9. Preliminary dye-trace study with submerged vane array.*

Summary data for all dye-trace experiments including average and standard deviation of length required to produce full vertical mixing or mass transport from the surface water to the channel bed are found in Tables B-6 and B-7 in Appendix B. Graphical representation on the increase in vertical mass transport, or vertical velocity (Eq. 4.6) is shown for all structures in Figures 10-14. Channel flow without submerged structures or under “clean flume” conditions were used to calculate vertical eddy diffusivity and length of vertical mass transport for water depths of 8, 10 and 12 inches at

a velocity of 0.8 ft/s. Friction velocity for the three water depths were 0.066, 0.073 and 0.800 ft/s respectively, for 8 to 10% of flow velocity. Vertical diffusion coefficients,  $\epsilon_v$ , and length of complete vertical mass transport,  $L_v$ , were both under and overestimated compared to steady state uniform flow conditions. It is hypothesized that the rectangular flume conditions with small width/depth ratio resulted in large wall effects. Theoretical vertical eddy diffusion,  $\epsilon_v$ , for water depths of 8, 10, 12-inches are 0.42, 0.59 and 0.77  $\text{in}^2/\text{s}$  while measured values were 1.7, 2.4, 3.6  $\text{in}^2/\text{s}$  respectively. This results in a length of complete vertical mass transport of 48.6, 34.8 and 26.5 feet compared to 15, 16.6, and 16.2 feet measured for different water depths. A calibrated coefficient,  $c_v$ , in Eq. 4.2 results in a values of 0.22, 0.18 and 0.16 for flow conditions at 8, 10 and 12-inches. These strongly resemble transverse eddy diffusions,  $c_t$ , (Chau, 2000; Fischer, 1979). However, if a 0.067  $c_v$  values is assumed the calibrated coefficient in Eq. 4.4 changes from 0.4 to 0.124, 0.185 and 0.245 for water depths of 8, 10, and 12-inches respectively, which is also similar to the transverse mixing coefficient of 0.1 Findings suggest rectangular flume vertical mixing, at experimental flow conditions of 0.8 ft/s, 8-12-inch water depth and 3-foot width, behave more closely to that of horizontal mixing due to the depth to width ratio. However, it is noted the length required to deliver complete vertical mixing only includes dye traces that presented strong vertical mass transport (80-90%), not solely molecular or small eddy diffusion.

The additional vertical mass transport observed through the introduction of structures such as boulders and stream barbs includes both turbulent and advective mixing. Due to strong flow experimental characteristics, structure analysis has been normalized over clean flume conditions. Data analysis for length of vertical mass transport include the use of Eq. 4.6 to determine the increase in vertical velocity,  $\Delta u_z$ , or VMT generated by various channel restoration structures, here presented in percent, %, over clean flume. Structures were found to all increase the rate of vertical velocity from 33% by a single boulder to 168% from a two-array vane system. Increase in vertical velocity,  $\Delta u_z$ , in percent has been plotted for all structure in Figures 10 to 13, with submergence ratio for a vane system in Figure 14.

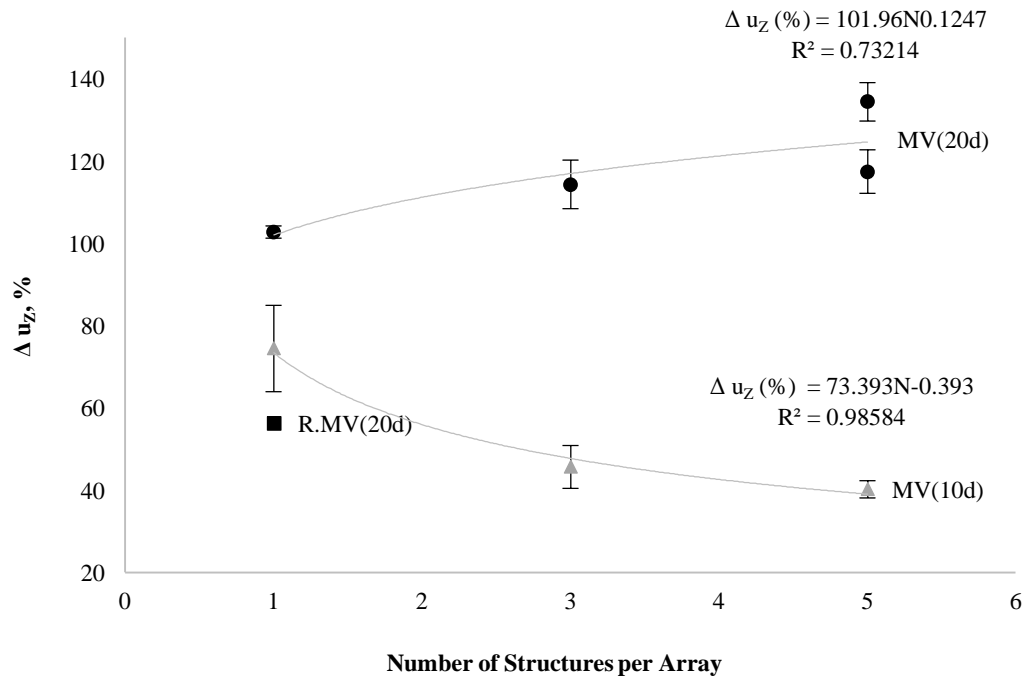


Figure 10. Increase in vertical velocity for single submerged vane array at various orientations.

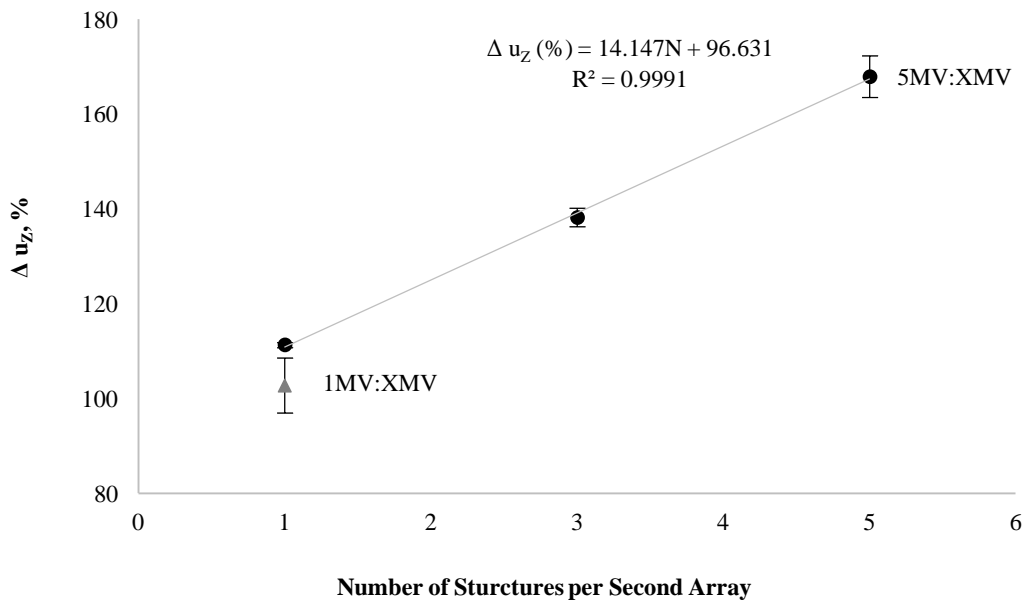


Figure 11. Increase in vertical velocity for two vane array system.

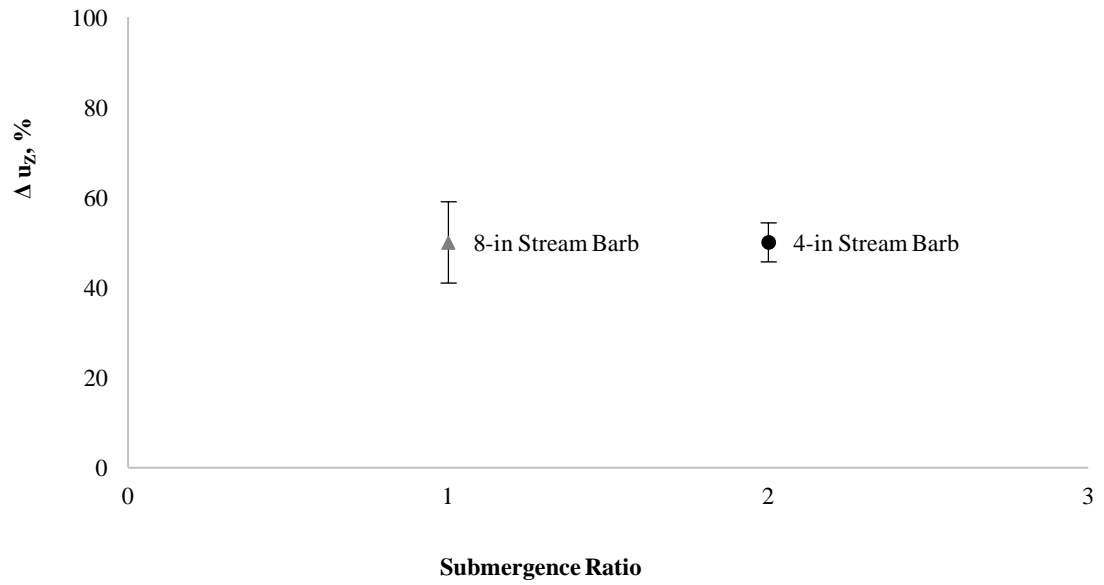


Figure 12. Increase in vertical velocity for single stream barb array.

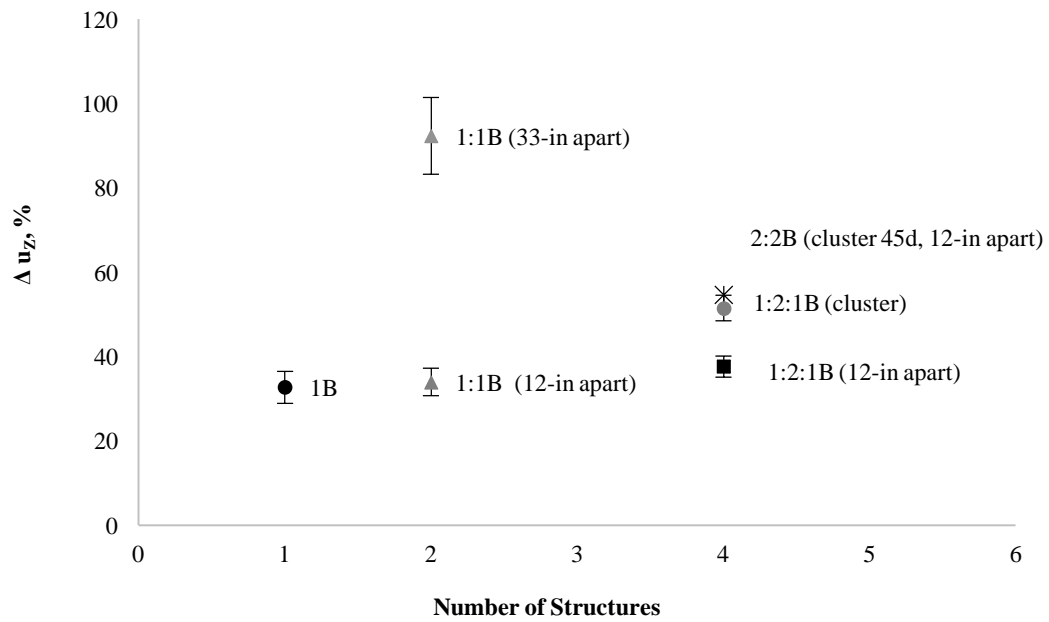


Figure 13. Increase in vertical velocity for boulders at various layouts.



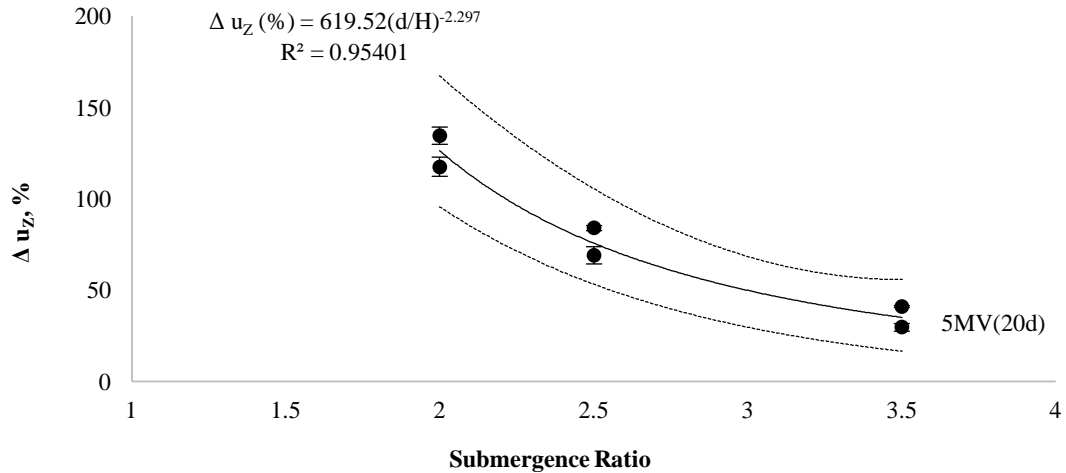


Figure 14. Submergence ratio effects on the increase in vertical velocity for submerged vane structures.

Single vane array consisting of 1, 3 and 5 structures per array were tested at 10 and 20 degrees, as well as a marble or rock covered vane at 20 degrees (Figure 10). Surprisingly, by increasing the number of vanes placed per array at 10 degrees reduced the rate of vertical mass transport, most likely caused by weak vortex generation and turbulent interference. However, a single vane at 10 degrees resulted in an over 74% increase in vertical velocity compared to clean flume conditions, while vanes at 20 degrees produced a 103% increase, compared to a marble covered 20-degree vane with 56%. With the addition in the number of vanes per array orientated at 20 degrees, the rate of vertical mass transport increased up to 134%, approximately equal to ten percent of stream wise velocity.

Multiple arrays of vanes were investigated at 10 and 20 degrees, with no additional increase in vertical velocity from 10-degree multiple array system. Vortex generation and flow coherence produced by an initial 5 vane array produced a linear increase in vertical mass transport followed by a 1, 3 or 5 vane array (Figure 11) up to 168% increase in vertical velocity over clean flume conditions. Results for boulders and stream barbs are displayed in Figures 12 and 13. It was found that both small and large stream barbs produced the same vertical mixing, with an increase in vertical velocity of 50 to 52%. Multiple orientations of boulders were tested, to gain a better understanding of cluster or spacing effects on boundary layer dynamics. Boulders are thought to

produce turbulence and high levels of mixing, however at a submergence ratio of that of vanes and the small stream barbs, ( $d/H = 2$ ), displayed little ability to facilitate vertical mass transport relative to clean flume conditions. The increase in rate of vertical velocity ranged from 33 to 55% (Figure 13). Improvements to vertical mass transport was achieved when two arrays of single boulder arrays were placed approximately 3-feet apart. This was accomplished due to the large disruption in upward curling boundary layer eddies by the second boulder due to wake turbulence generated by the first boulder.

Submergence ratio is importance when determining the capacity to induce vertical mixing. Figure 14 shows how the rate of vertical mass transport decreased when submergence ratio increased from 2 to 3.4 (5-array vane system at 20 degrees). Relative to the clean flume conditions, the increase in vertical velocity dropped from 120% to 35%. In all these cases the flow velocity maintained constant at 0.8 ft/s. Ninety percent confidence interval is plotted for the two experiments per submergence ratio.

#### **4.6 Summary**

In channel flow without structures, vertical mass transfer occurs as a result of turbulent and molecular dispersion. Submerged structures introduced in the line of flow provide additional advection, which enhances dispersion and vertical mass transfer. In the case of vanes, vertical mass transfer is further increased by horizontal circulation or vorticity, while in the case of blocks and boulders, the mass transfer is dominated by turbulent dispersion. Stream barbs with their tetrahedron design provide flow redirection from bottom to top of the channel with turbulent wave generation. Vertical mass transport results from centerline dye-trace study indicate that a system of vanes (angled at 20-degrees) create a rate of vertical mass transfer increased by 100% compared to only a 50% increase for stream barbs with similar energy loss or backwater effects. Stream barbs were effective in vertical mass transport due the sloped sides. It was observed that if boulders are to be used for the purpose of inducing vertical mass transport a larger spacing of several feet should be used to reduce boundary layer interference.

## **CHAPTER 5.**

### **CONCLUSIONS, ENGINEERING SIGNIFICANCE AND FUTURE RESEARCH**

#### **5.1 Energy Loss and Vertical Mass Transport Study Conclusions**

The motivation for the two sets of studies was to (1) compare the energy loss associated with different channel restoration structures and (2) evaluate the efficiency of the structures in producing vertical mass transport. Theoretical energy loss relationships were developed, compared, and evaluated experimentally for stream barbs, spurs, submerged vanes, blocks and boulders. Extensive preliminary dye-trace analyses were conducted on all structures tested using non-buoyant dye tests were conducted to determine length of complete vertical mixing for various layouts of stream barbs, vanes and boulders. Submerged structures were placed below or at the water depth. Most tested were constructed at a submergence of the structures were half the water depth, however stream barb design recommendations of water depth height were evaluated. Vertical mass transport capabilities were evaluated for the same flow conditions, with additional submergence ratio tests on a submerged vane system. Both theory and measurements show that vane systems accomplish efficient mass transfer with complete mixing at considerably less energy loss than do the corresponding system of equivalent blocks, boulders and/or barbs.

Submerged vanes angled more than 20 degrees were shown to significantly increase both energy expenditure and vertical mass transport due to flow separation behind the structure. Stream barbs were not found to stimulate elevated levels of drag force and backwater effect when aligned on the bank, due to the channelization of flow, and compared to theoretical estimations with only small observed changed in drag coefficients under experimental conditions from 0.9 to 0.75 and 0.5 for large and small barb systems respectively. Small spur and wall attached vane systems displayed increased energy loss compared to barbs, suggesting the side slope of 45-degrees in the stream barb design effectively redirects flow with vertical mass transport similar to many

boulder configurations. Drag coefficient for vertical spur system with equivalent stream barb at half the water depth was greatly reduced over theoretical relationships to 0.85 from 1.4. Energy expenditure on a two boulder array system resulted in increased energy loss; drag coefficients ranging from 3.1 to 1.9 for spaced systems. This is more than three times that compared to theoretical drag coefficient of 0.6 for a hemispherical object. Further studies are needed at different layouts to determine if the findings include blockage. Multiple boulder spacing and design clusters were evaluated for vertical mass transport capabilities. Efficient vertical mass transport was achieved with two single-boulder array spaced approximately 3-feet apart. These results suggest that if energy slope is a critical aspect of a channel restoration project, submerged vanes could be a viable and attractive alternative to rock and boulder structure. As has been shown the vortex forcing produced by closely spaced submerged vane array system results in coherent longitudinal vortices and efficient mixing with minimal energy loss.

Table 4. Increase in vertical velocity (VMT) compared to estimated energy loss (BWE).

	$\Delta U_z$ , %	$\Delta S$ , % ( $10^3$ )	Normalized Ratio
1 MV(10d)	74	0.33	165,900
3 MV(10d)	46	0.98	40,400
5 MV(10d)	40	1.63	23,800
1 MV(20d)	103	1.04	84,200
3 MV(20d)	114	3.13	34,600
5 MV(20d)	126	5.22	24,100
1:1 MV(20d)	103	1.49	67,700
5:1 MV(20d)	111	8.95	12,400
5:3 MV(20d)	138	23.86	5,800
5:5 MV(20d)	168	89.45	1,900
1 Boulder	33	1.46	17,400
1:1 Boulder	92	4.75	15,500
4-in Stream Barb	50	1.63	30,400
8-in Rock Barb	50	4.88	10,000

Theoretical energy loss relationships for structures have been calibrated under experimental flow conditions, and compared to the ability for a structure to increase

vertical mass transport through additional advective or turbulent vertical motion, including length and occurrence of complete vertical mixing,  $L_x$ . Table 4 displays the increase in vertical velocity,  $u_z$ , using Eq. 4.6, and estimated change in slope of friction as calculated for each design using Eqs. 3.5, 3.8, 3.9 and 3.10. The ratio of the increase in vertical velocity, or vertical mass transport, to backwater effect has been presented to directly compare percent increase in vertical velocity,  $\Delta U_z$ , to percent increase in the slope of the channel,  $\Delta S$ , produced by the addition of such structures, under experimental flow conditions. Ratio of  $\Delta U_z/\Delta S$  has been normalized of the rate of occurrence of complete vertical mass transport observed in dye-trace studies.

Table 5. Shear velocity, vertical diffusivity, and length of vertical mass transport compared to experimental measurements.

	$u^*$ , in/s	$\epsilon_y$ , in <sup>2</sup> /s	$L_x$ , est. ft	$L_x$ , exp. ft
Clean Flume	0.8	0.4	15.0	15.0
1 MV(10d)	0.8	0.4	14.9	8.6
3 MV(10d)	0.8	0.4	14.6	10.3
5 MV(10d)	0.8	0.4	14.4	10.7
1 MV(20d)	0.8	0.4	14.7	7.4
3 MV(20d)	0.8	0.5	14.0	7.0
5 MV(20d)	0.9	0.5	13.4	6.5
1:1 MV(20d)	0.8	0.4	14.5	7.4
5:1 MV(20d)	0.9	0.5	12.5	7.1
5:3 MV(20d)	1.2	0.6	10.1	6.3
5:5 MV(20d)	1.8	1.0	6.4	5.6
1 Boulder	0.8	0.4	14.5	11.3
1:1 Boulder	0.9	0.5	13.5	7.8
4-in Stream Barb	0.8	0.4	14.4	10.0
8-in stream Barb	0.9	0.5	13.5	10.0

The research presented in this thesis illustrates that the use of dispersion relationships to estimate length of vertical mass transport based on energy slope and estimated shear velocity of the channel does not properly correct for advection and angular motion produced by channel restoration structures. As mentioned, such systems would need to be further evaluated using an Acoustic Doppler Velocimeter (AVD) device, which was not the focus of this research. Several empirical relationships and

experimental methods have been developed to determine environmental fluid dynamics in streams and rivers, the equations used include established and general conclusions on shear velocity, length of complete vertical mixing and average vertical velocity. Vertical mixing equations were evaluated using energy loss and vertical mass transport data from both studies, and the adjusted coefficient of 0.124 rather than 0.4 (Eq. 4.4) for use in determining shear velocity to compare estimated and experimental length of complete vertical mixing (Eqs. 4.1, 4.2 and 4.4) in Table 5. As can be seen, submerged vanes angled at 20-degrees result in an overestimation in mixing length determined by channel restoration structure induce slope of friction, as well as a single submerged vane at 10-degrees and a two array boulder field. All channel restoration structures tested provide high levels of temporary roughness on the stream flow resulting in efficient vertical mixing compared to that achievable from uniform roughness stream bed frictional forces.

## **5.2 Engineering Significance**

Physical based modeling was performed on multiple channel restoration structures of different designs and orientations to quantify their ability to produce backwater and vertical mass transport. Several contemporary issues that suggest the importance of research on engineered channel restoration structures include the deterioration of surface water quality and the growing risk of high runoff events and flooding. The deterioration of streams and surface water quality continues despite channel restoration efforts and reduction in point and non-point source contamination. The EPA's *National Water Quality Inventory* under section 305(b) of the Clean Water Act assessed 563,955 miles of U.S. rivers and streams (16% of the total 3.5 million). Impaired conditions limiting human and environmental benefit was found in 44% of those assessed, with 53% 'good' condition and 3% 'threatened' (U.S. EPA, 2009). Pathogens were found to be the leading cause of impairment followed by habitat loss, and low dissolved oxygen concentrations. Origin of impairment were largely identified as the consequences of agricultural activities, hydro-modifications (i.e. water diversions, channelization, and dam construction) followed by unknown causes, habitat alteration,

natural/wildlife, municipal discharge and sewage, nonpoint source, atmospheric deposition, resource extraction and storm water runoff. Similar trends have been shown in previous National Water Quality Inventory Reports (2015). The ecological and political importance for the advancement of channel restoration technologies and efforts are highly stressed in the review *Ecological Restoration of Streams and Rivers: Shifting Strategies and Shifting Goals* by Palmer et al (2014). The fact that the United States Clean Water Act state's the goal "to restore and maintain the chemical, physical and biological integrity of the Nation's water" suggest that the need for improvement of our water ways with effective and highly designed technologies is necessary. Additionally, within the past few decades, changes in the hydrological cycle have seen an increasingly occurrence of drought periods as well as large storm events resulting in large fluctuations in stream flow leading to bank instability and soil loss causing degradation of stream integrity. The demand for channel restoration structures for the purposes of bank protection and stabilization, with emphasis on vertical mass transport and water quality improvements, may become more important as communities reach for less intrusive, economical, and environmentally friendly solutions. The research conducted in these two studies have provided data for a select number of such structures.

### **5.3 Future Research**

This thesis comprises research performed to determine head loss and mixing characteristics of existing stream restoration structures. Experiments were limited to a single flow condition given the number of designs and layouts tested. Flow rate was maintained at 1.6 ft<sup>3</sup>/s, at 8-inches water depth velocity at 0.8 ft/s and slope at 0.02%. Supplementary tests were conducted at depths of flow of ten and twelve inches to determine submergence ratio effects on structure induced vertical mass transfer. More tests are needed to evaluate the effect of flow velocity and depth on drag coefficients and efficiency factors. Spacing design should be further tested on stream barbs and boulders. Additional variations in structure layout for large boulders should be investigated to further develop energy loss and vertical mass transport relationships. The use of the

vertical mass transport to backwater effect ratio in this thesis was presented for ease of comparison. A similar normalization could be done for other channel restoration goals, as well including field observations. Stream restoration projects are underway across the country requiring large economic, construction, and engineering demand for improved design standards and guidelines. Through the integration of direct numerical evaluation of structure design and orientation under physical based modeling, greater assurance can be made to the improved efficiency and effectiveness of such structures.



## REFERENCES

- Anderson, J.D. (2008). Introduction to Flight. 6th Ed., McGraw Hill, New York, ISBN 0-07-126318-7.
- Azinfar, H., and Kells, J.A. (2009). "Flow resistance due to a single spur dike in an open channel." Journal of Hydraulic Research, 47(6), 755-763.
- Battin, T.J., Kaplan, L.A., Newbold, J.D., Cheng, X., and Hansen, C. (2003). "Effects of Current Velocity on the Nascent Architecture of Stream Microbial Biofilms." Applied and Environmental Microbiology, 69(9), 5443-5452.
- Belayneh, Moltot Zewdie, and Sreenivasa Murty Bhallamudi. "Optimization Model for Management of Water Quality in a Tidal River Using Upstream Releases." JWARP Journal of Water Resource and Protection 04.03 (2012): 149-62. Web.
- Besemer, K., Singer, G., Hodl, I. and Battin, J.T. (2009). "Bacterial Community Composition of Stream Biofilms in Spatially Variable-Flow Environments." Applied and Environmental Microbiology, 75(22), 7189-7195.
- Bernard, Jerry M., and Ronald W. Tuttle. "Stream Corridor Restoration: Principles, Processes, and Practices." *Engineering Approaches to Ecosystem Restoration* (1998).
- Bernhardt, E. S., M. A. Palmer, J. D. Allan, G. Alexander, K. Barnas, S. Brooks, et al. (2005). Synthesizing U.S. river restoration efforts. Science 308:636-637.
- Blevins, R.D. (2003). Applied Fluid Dynamics Handbook. Van Nostrand Reinhold Company, Inc., New York.
- Cabral, João P. S. "Water Microbiology. Bacterial Pathogens and Water." International Journal of Environmental Research and Public Health IJERPH 7.10 (2010): 3657-703. Web.
- Chau, K.w. "Transverse Mixing Coefficient Measurements in an Open Rectangular Channel." Advances in Environmental Research 4.4 (2000): 287-94.
- Davidson, P. (2015). Turbulence: An Introduction for Scientists and Engineers (2 ed.). Oxford, United Kingdom: Oxford University Press.
- Davis, Mackenzie Leo, and Susan J. Masten. *Principles of Environmental Engineering and Science*. New York, NY: McGraw-Hill, (2004). ISBN 0-07-235053-9.
- Devkota, Bishnu H., and Jörg Imberger. (2009). "Lagrangian Modeling of Advection-diffusion Transport in Open Channel Flow." Water Resources Research 45, W12406, doi:10.1029/2009WR008364.
- Espigares M, Coca C, Fernández-Crehuet M, Moreno O, Gálvez R. Chemical and Microbiologic Indicators of Fecal Contamination in the Guadalquivir (Spain) Eur. Water Pollut. Control. (1996). 6:7-13.
- EPA. (2015). Water: Best Management Practices Riparian/Forested Buffer. (U. S. Agency, Producer) Retrieved from [water.epa.gov:http://water.epa.gov/polwaste/npdes/swbmp/Riparian-Forested-Buffer.cfm](http://water.epa.gov/polwaste/npdes/swbmp/Riparian-Forested-Buffer.cfm).
- EPA. (2015). Water: Stage 2 DBP Rule. (United States Environmental Protection Agency) Retrieved from [water.epa.gov: http://water.epa.gov/lawsregs/rulesregs/sdwa/stage2/basicinformation.cfm](http://water.epa.gov/lawsregs/rulesregs/sdwa/stage2/basicinformation.cfm).

Fischer, Hugo B., E. John List, Robert C.Y. Koh, Jorg Imberger, and Norman H. Brooks. *Mixing in Inland and Coastal Waters*. New York: Academic, 1979. Print.

Franks, F. *Water - a Comprehensive Treatise*. Volume 1. *The Physics and Physical Chemistry of Water*. New York, NY: Plenum, 1972. Print.

Geographic Information System Analysis of the Surface Drinking Water Provided by Intermittent, Ephemeral and Headwater Streams in the U.S. Environmental Protection Agency. Unilever Research Laboratory. (1972).

Gualtieri, Carlo, Paola Gualtieri, Guelfo Pulci Doria, and Charles S. Melching. "Reaeration Equations Derived from U.S. Geological Survey Database." *J. Environ. Eng. Journal of Environmental Engineering* 126.12 (2000): 1159-160.

Hamuy-Blanco, A. and James, C.S. (2014). "Enhancement of habitat heterogeneity by placement of boulders in streams." *River Flow 2014, International Conference on Fluvial Hydraulics*, Schleiss et al. (Eds.), 2014 Taylor & Francis Group, London, ISBN 978-1-138-02674-2, pp. 2321-2329.

Higashino, M., and Stefan, H.G. (2011). "Dissolved Oxygen Demand at the Sediment-Water Interface of a Stream: Near-Bed Turbulence and Pore Water Flow Effects." *Journal of Environmental Engineering*, 137(7), 531-540.

Hellweger, F. L. (2015). 100 Years since Streeter and Phelps: it is time to update the biology in our water quality models. *Environmental Science and Technology*, 49, 6372- 6373.

Hossein Azinfar, J. A. (2011). Drag force and associated backwater effect due to an open channel spur dike field. *Journal of Hydraulic Research*, 49 (2), 248-256.

IDNR. (2010). *Iowa Surface Water Quality Standards Implementation*. Iowa Department of Natural Resources, Water Resources Section.

Ji, Zhen-Gang. *Hydrodynamics and Water Quality: Modeling Rivers, Lakes, and Estuaries*. Hoboken, NJ: Wiley- Interscience, 2008. Print.

"National Water Quality Inventory: Report to Congress." 2004 Reporting Cycle. Environmental Protection Agency (EPA 841-R-08-00). January 2009.

"National Water Quality Inventory Report to Congress." EPA. Environmental Protection Agency, (2015) <<https://www.epa.gov/waterdata/national-water-quality-inventory-report-congress>>.

Nezu, Iehisa. "Open-Channel Flow Turbulence and Its Research Prospect in the 21st Century." *Journal of Hydraulic Engineering J. Hydraul. Eng.* 131.4 (2005): 229-46. Web.

NRCS (2007). *Stream Restoration Design Handbook*, National Engineering Handbook, Part 654, Washington, D.C.

Maddock, Ian, Atle Harby, Paul Kemp, and Paul J. Wood. *Ecohydraulics: An Integrated Approach*. Chichester: John Wiley & Sons, 2013. Print.

Makota Higashino, H. G. (2011). Dissolved Oxygen Demand at the Sediment-Water Interface of a Stream: Near Bed Turbulence and Pore Water Flow Effects. *Journal of Environmental Engineering*, 137 (7), 531-540.

Maupin, M.A., Kenny, J.F., Hutson, S.S., Lovelace, J.K., Barber, N.L., and Linsey, K.S., 2014, Estimated use of water in the United States in 2010: U.S. Geological Survey Circular 1405, 56 p., <<http://dx.doi.org/10.3133/cir1405>>.

Miller, Scott W., Phaedra Budy, and John C. Schmidt. "Quantifying Macroinvertebrate Responses to In-Stream Habitat Restoration: Applications of Meta-Analysis to River Restoration." *Restoration Ecology* 18.1 (2010): 8-19.

Mixing in Rivers: Turbulent Diffusion and Dispersion. Karlsruhe Institute of Technology (KIT), Institute for Hydromechanics. Karlsruhe: University of the State of Baden- Wuettemberg and National Research Center of the Helmholtz Association.

Odgaard, A. J., and Mosconi, C.E. (1987). "Streambank protection by submerged vanes." *Journal of Hydraulic Engineering* 113(4), 520-536. Odgaard, A. J. and Wang, Y. (1991).

Odgaard A. J., and Wang, Y. (1991). "Sediment Management with Submerged Vanes. I: Theory." *Journal of Hydraulic Engineering*, 117(3), 267-283.

Odgaard, A. J. and Spoljaric, A. (1989). "Sediment control by submerged vanes. Design basis." *River meandering*. S. Ikeda and G. Parker, eds., Water Resources Monograph No. 12, American Geophysical Union, 127-151.

Odgaard, A. J. and Snyder, K, and Barquist, B. (2016). "Energy Loss from Difference Channel Restoration Structures." *River Flow*, St. Louis, Missouri. July 12<sup>th</sup>. Unpublished conference paper. IAHR Fluvial Hydraulics Committee, 2016. Print.

Odgaard, A. J. and Snyder, K and Barquist, B. (2016). "Energy Loss from Difference Bank Protection Structures." *World Environmental and Water Resources Congress*, West Palm Beach, Florida, May 22<sup>nd</sup>. Unpublished conference paper. American Society of Civil Engineers, Virginia, 2016. Print.

Odgaard, A. J. (2009). *River Training and Sediment Management with Submerged Vanes*. ASCE Press. Reston, VA.

Palmer, Margaret A., Kelly L. Hondula, and Benjamin J. Koch. "Ecological Restoration of Streams and Rivers: Shifting Strategies and Shifting Goals." *Annu. Rev. Ecol. Evol. Syst. Annual Review of Ecology, Evolution, and Systematics* 45.1 (2014): 247-69.

S. A. A. Mamun Hossain, A. K. (2013). Stream Barb Influenced on Straight Channel Bed Configuration: A Numerical Simulation. *Journal of Environmental Science and Natural Resources*, 6 (2), 139-147.

Sabersky, R.H., and Acosta, A. J. (1964). *Fluid Flow*. Mac Millan Publishing Co., Inc., New York, N.Y.

Small, M. J., and M. W. Doyle. "Historical Perspectives on River Restoration Design in the USA." *Progress in Physical Geography* 36.2 (2011): 138-53.

Socolofsky SA, Jirka GH (2004) Special topics in mixing and transport processes in the environment. Texas AM University, College Station, pp 51–80.

Southard, J. (2006). *Introduction to Fluid Motions, Sediment Transport, and Current Generated Sedimentary Structures*. Course Notes, MIT, Earth Atmospheric and Planetary Sciences.

"Studies Linking the Construction of Instream Structures to Increases in Flood Levels." *Upper Mississippi River Restoration*. Nicollet Island Coalition, (2014) <<http://www.wv.nicolletislandcoalition.org/wp-content/uploads/sites/7/2015/01/List-of-Studies-linking-RTS-to-flooding.pdf?c0793e>>.

Stull, R. B. (1994). *An Introduction to Boundary Layer Meteorology*. Madison, Wisconsin, U.S.A: Kluwer Academic Publishers. U.S. EPA. (2009).

"Summary of Research on the Effects of River Training Structures on Flood Levels." *Applied River Engineering Center, U.S. Army Corps of Engineers - St. Louis District, (2014)*.

Wang, Y. and Odgaard J. A. (1991). *Sediment Control with Submerged Vanes*. University of Iowa, Civil and Environmental Engineering. Iowa City: Graduate College.

Wang, Y. and Odgaard, A. J. (1993). "Flow control with vorticity." *Journal of Hydraulic Research*, 31(4), 549-562.

## APPENDIX A. PHYSICAL MODEL DIAGRAMS AND PICTURES

### A.1 Titled Flume

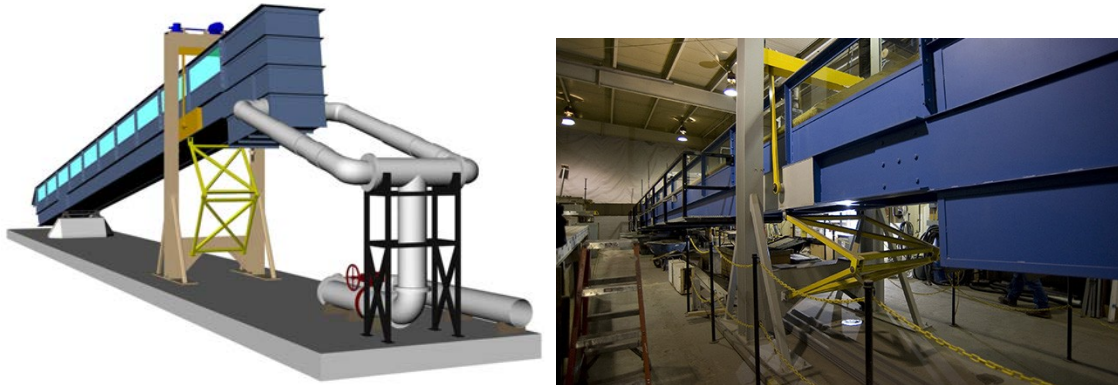


Figure A-1. IIHR's Tilted flume, a three-foot-wide rectangular flume with length of 54 feet.

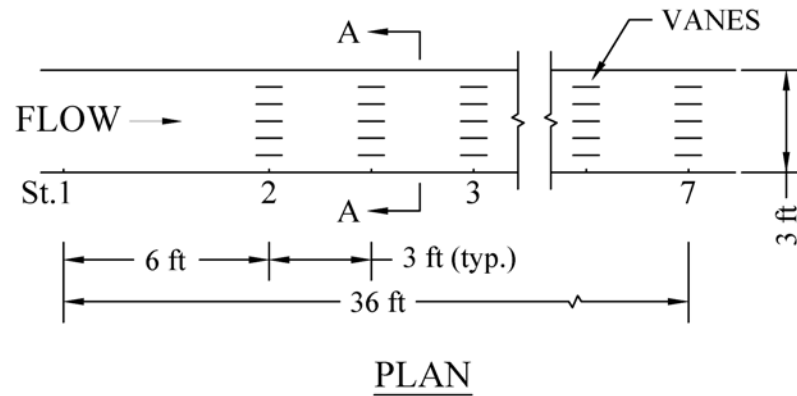
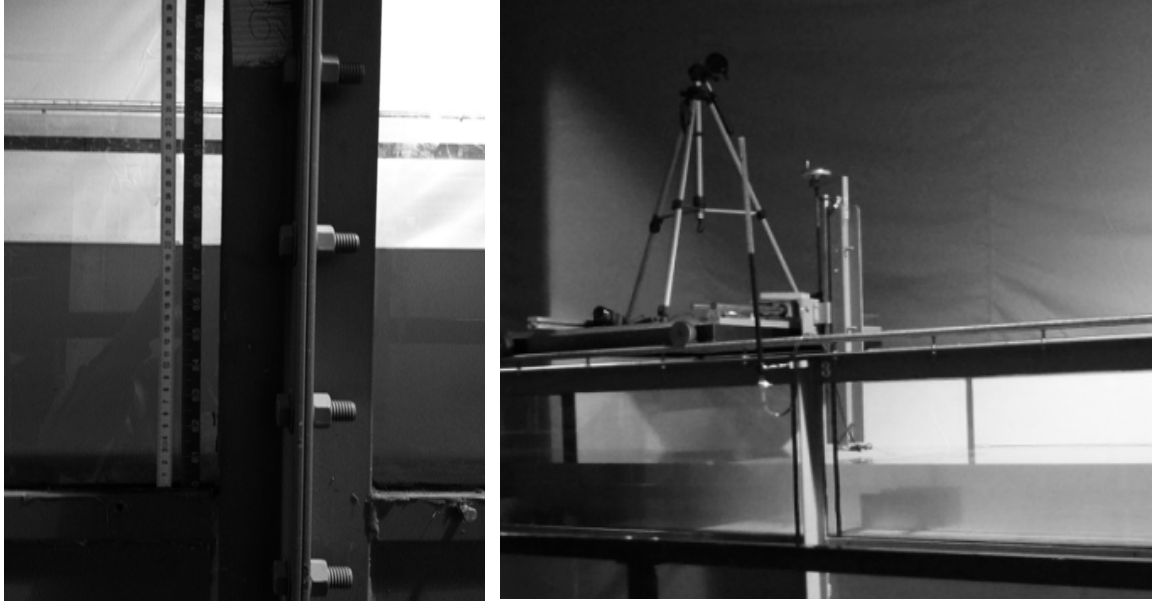
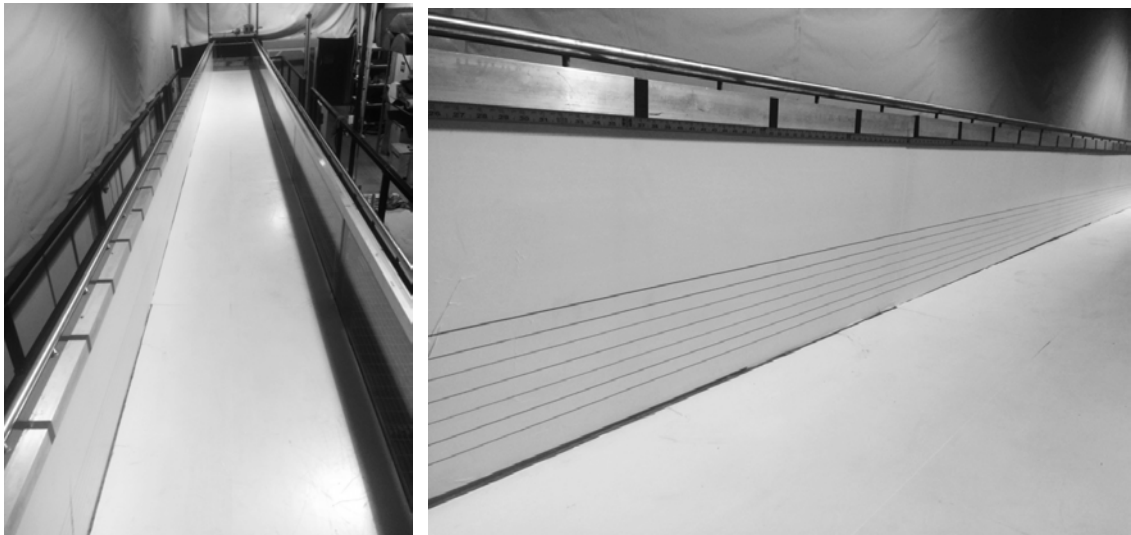


Figure A-2. Plane view of experimental set-up on IIHR's Tilted Flume.



*Figure A-3. Laboratory experimental set-up of backwater effect measurement devices (Left) and vertical mass transport dye tracer device (Right).*



*Figure A-4. Flume sheeted covering and lining system utilized in vertical mass transport dye tracer investigations.*

## A.2 Channel Restoration Structure Design

### Stream Barbs

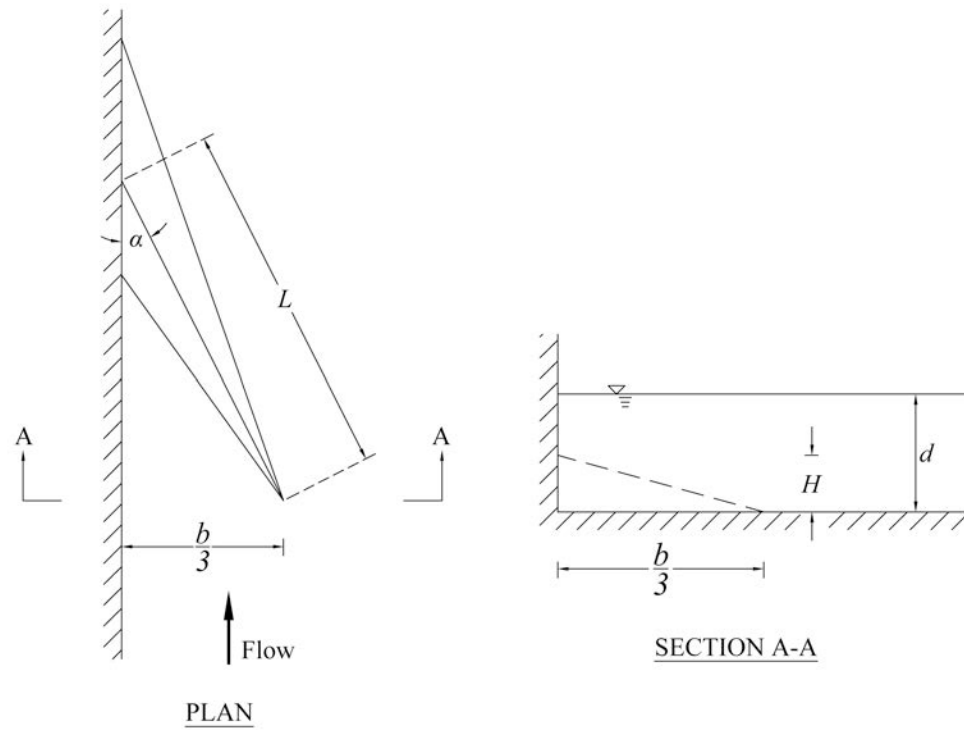
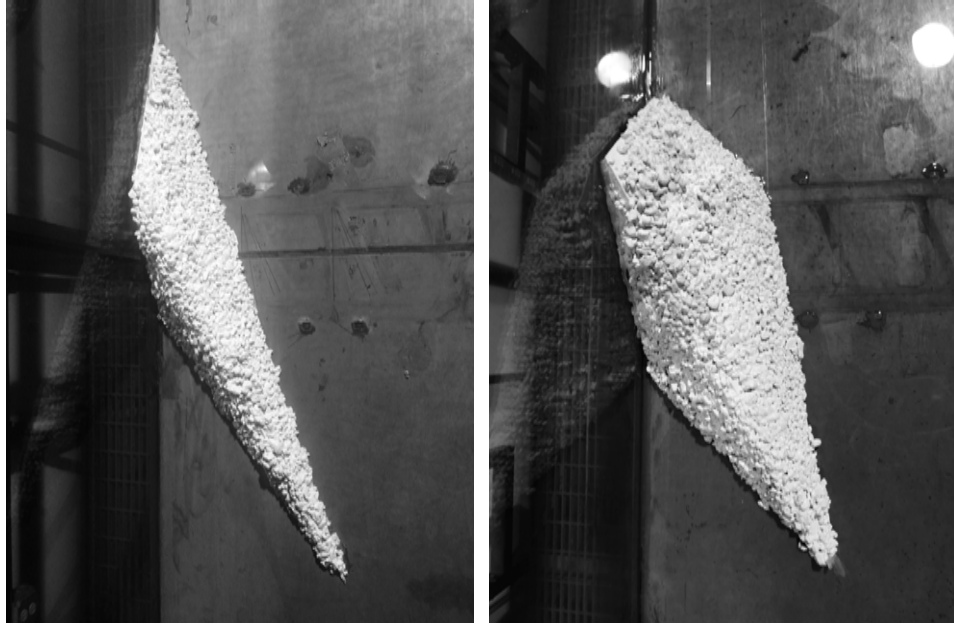


Figure A-5. Backwater and vertical mass transport plan and elevation diagram for stream barb ( $H=d/2 = 4$ -inches shown). Both designs angled at 27 degrees.





*Figure A-6. Plan view of actual stream barb structures, small stream barb and large stream barb.*



*Figure A-7. Stream Barb array used in backwater effect study.*



## Spur

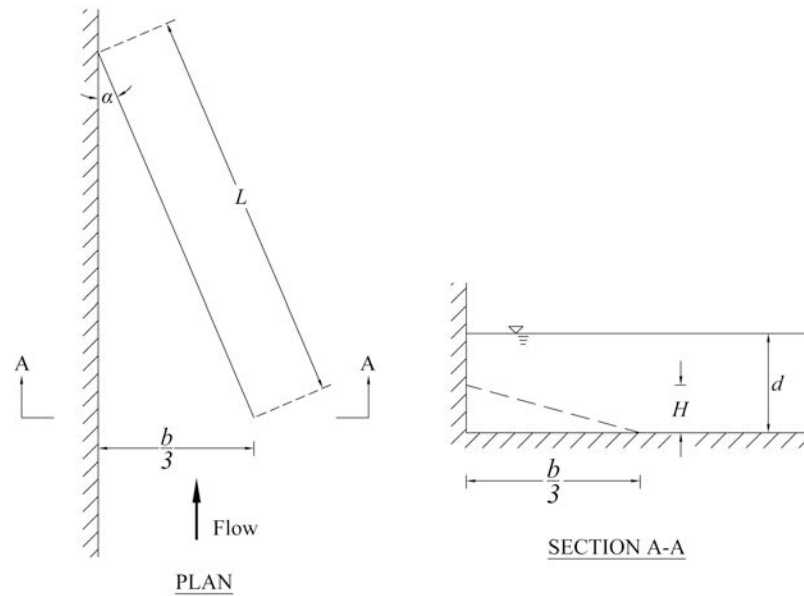


Figure A-8. Backwater study plan and elevation diagram spur ( $H=d/2 = 4$ -inches shown). Structures are angled at 27 degrees into the direction of flow.



Figure A-9. Spur array used in backwater effect study.

## Vane – Wall System

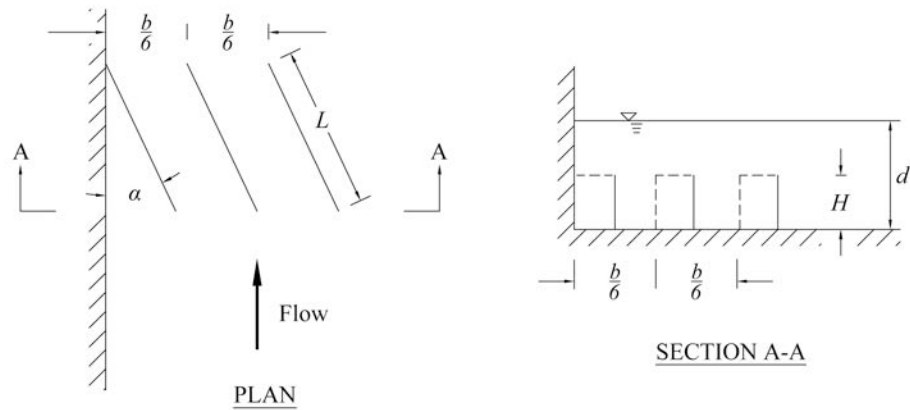
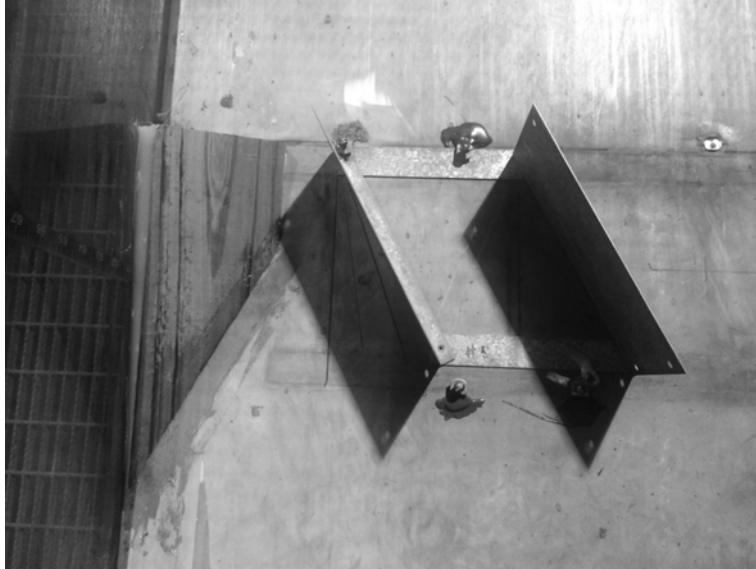


Figure A-10. Vane – wall structure backwater study plan and elevation diagram. Structures are angled at 20 degrees into the direction of flow.

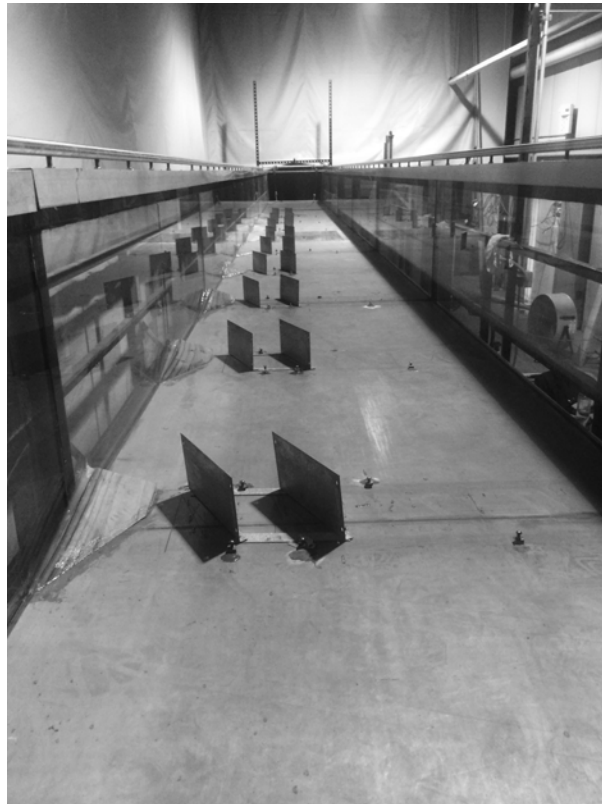


Figure A-11. Vane – wall system used in backwater effect study, angled at 20-degrees. Also known as the vane spur combination. Note: Picture taken from downstream looking upstream.

## Vane – Ramp System



*Figure A-12. Plan view of metal vane - ramp system used in backwater effect study.*



*Figure A-13. Metal vane – ramp system used in backwater effect study.*

## Metal Vanes, Blocks and Frontal Projections

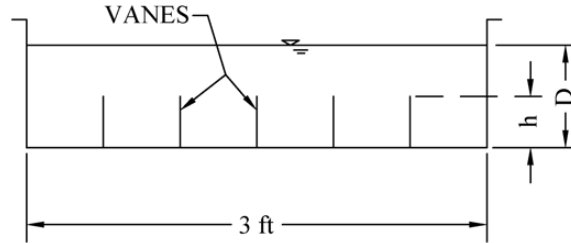


Figure A-14. Metal vane array structure backwater and vertical mass transport plan and elevation diagram.

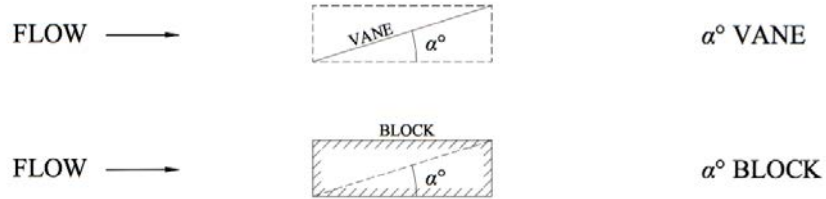


Figure A-15. Plan view of metal vane and block equivalents given angle of attack.

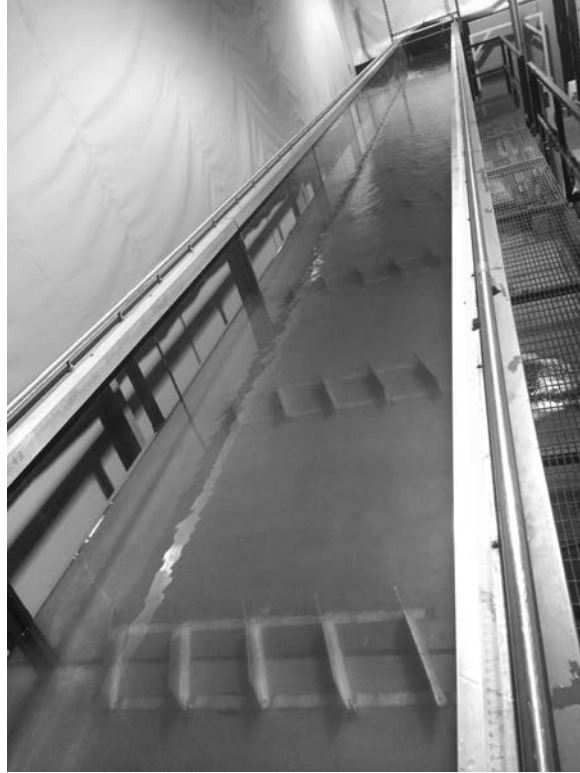


Figure A-16. Metal vane and equivalent full block and frontal projections used in backwater effect study.

## Boulders



*Figure A-17. Boulders or hemisphere blocks used in backwater effect study.*

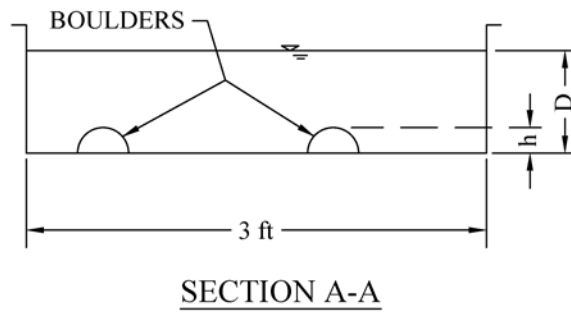
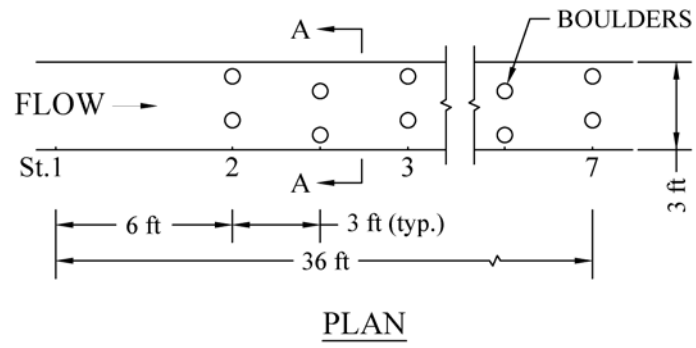


Figure A-18. Two boulder array structure backwater study plan and elevation diagram.

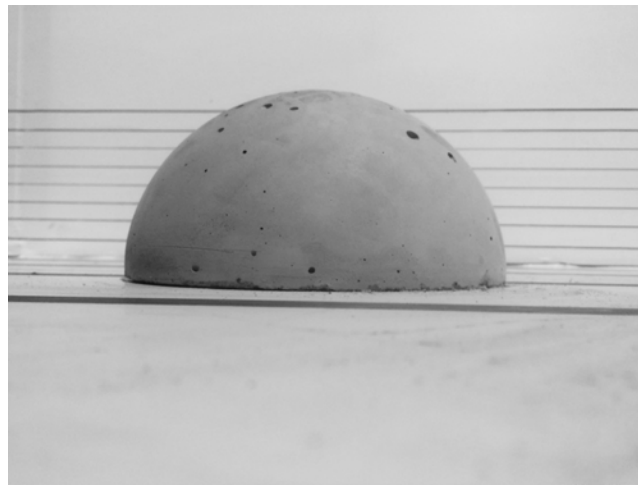
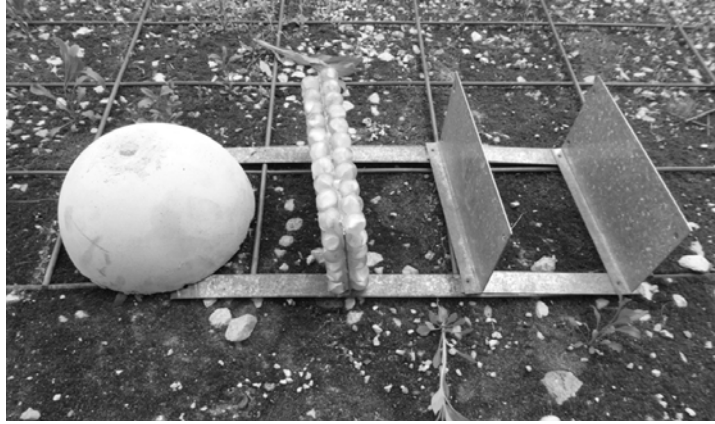


Figure A-19. Boulder structure used in backwater effect and vertical mass transport study.



### A.3 Vertical Mass Transport



*Figure A-20. Boulder, marbles covered naturalized vane and metal vane structures.*

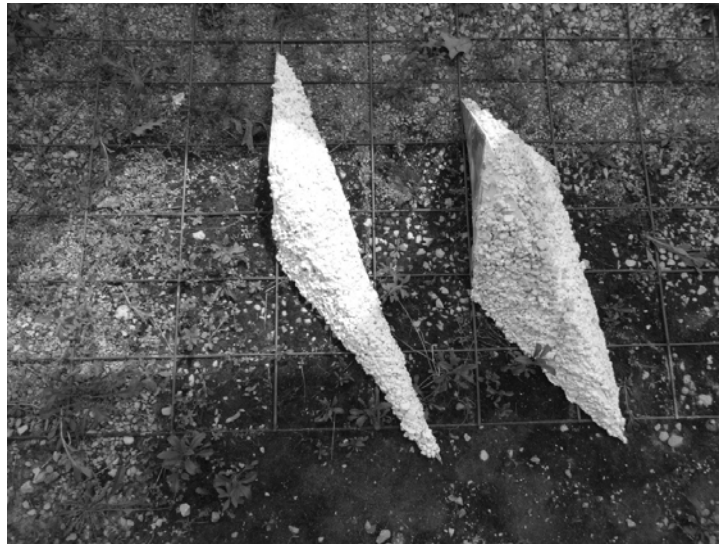


*Figure A-21. Small and large stream barb structures.*



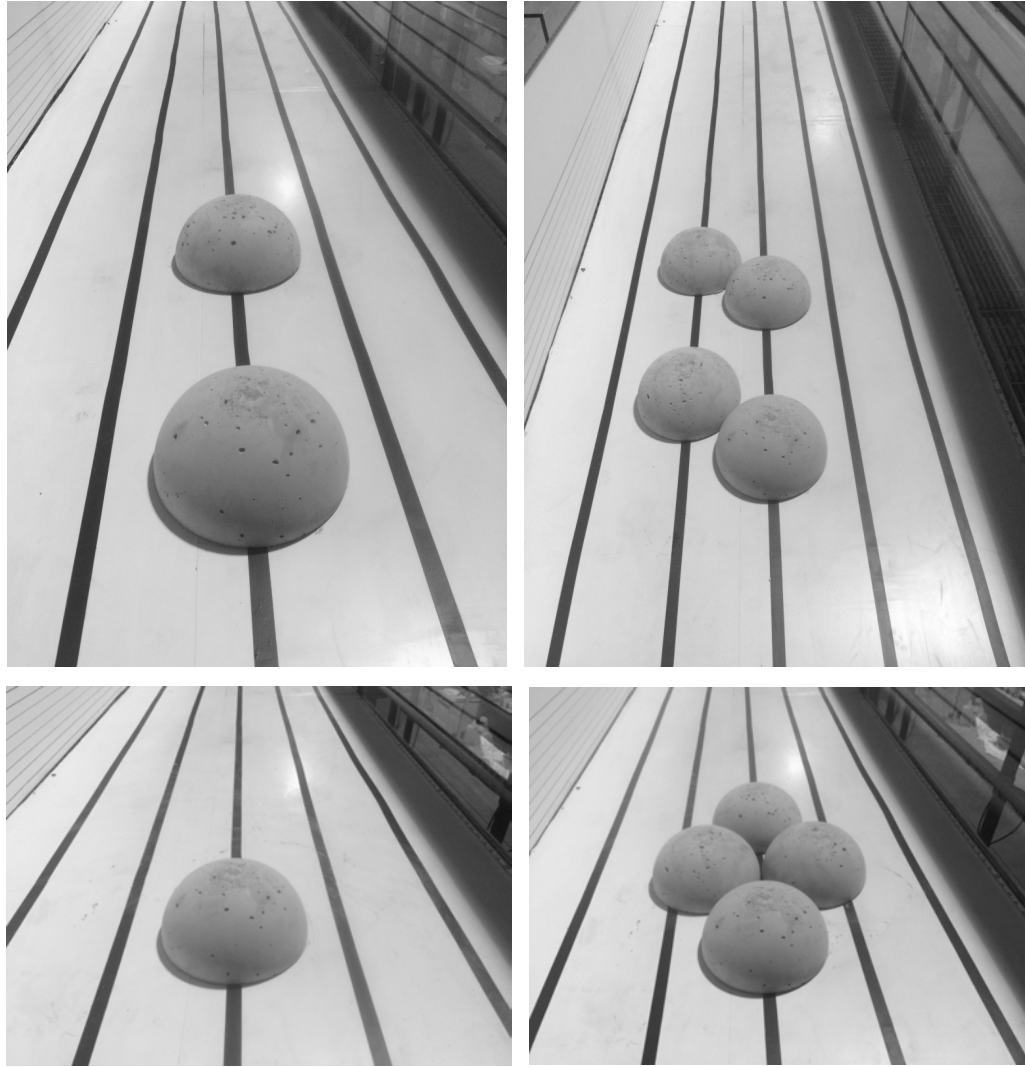


*Figure A-22. Vertical mass transport study; boulder design orientations, including (Top) two arrays of single boulders, two arrays of two boulders angles at 45-degrees, (Bottom) single boulder, and 4 boulder cluster.*

## APPENDIX B. EXPERIMENTAL DATA

### B.1 Backwater Effect and Energy Loss Measurements

*Table B-1. BWE change in depth in inches for submerged vanes, 11 sets.*

<i>Section</i>	<i>1</i>	<i>2</i>	<i>3</i>	<i>4</i>	<i>5</i>	<i>6</i>	<i>7</i>
<i>0 Degrees</i>	0.04	0.02	0.01	0.02	0.00	-0.01	0.00
<i>5 Degrees</i>	0.02	0.02	0.02	0.02	0.01	-0.02	0.00
<i>10 Degrees</i>	0.06	0.03	0.04	0.03	0.02	-0.01	0.00
<i>15 Degrees</i>	0.08	0.07	0.08	0.05	0.04	0.01	0.00
<i>20 Degrees</i>	0.16	0.11	0.13	0.09	0.05	0.01	0.00
<i>25 Degrees</i>	0.34	0.24	0.23	0.17	0.12	0.05	0.00

*Table B-2. BWE change in depth in inches for vane and vane equivalents.*

<i>Section</i>	<i>1</i>	<i>2</i>	<i>3</i>	<i>4</i>	<i>5</i>	<i>6</i>	<i>7</i>
<i>10 Deg. Metal Vanes 11 Sets</i>	0.06	0.03	0.04	0.03	0.02	-0.01	0.00
<i>10 Deg. Metal Vanes 6 Sets</i>	0.04	0.03	0.03	0.02	0.01	-0.02	0.00
<i>10 Deg. Frontal Projection, As</i>	0.22	0.19	0.15	0.11	0.07	0.03	0.00
<i>10 Deg. Full Blocks/Boulders</i>	0.18	0.14	0.10	0.09	0.05	0.01	0.00
<i>20 Deg. Metal Vanes 11 Sets</i>	0.16	0.11	0.13	0.09	0.05	0.01	0.00
<i>20 Deg. Metal Vanes 6 Sets</i>	0.11	0.06	0.08	0.06	0.05	0.00	0.00
<i>20 Deg. Frontal Projection, As</i>	0.56	0.46	0.40	0.31	0.19	0.09	0.00
<i>20 Deg. Full Blocks/Boulders</i>	0.40	0.32	0.24	0.18	0.12	0.05	0.00
<i>25 Deg. Metal Vanes 11 Sets</i>	0.34	0.24	0.23	0.17	0.12	0.05	0.00
<i>25 Deg. Full Blocks/Boulders</i>	0.70	0.56	0.44	0.36	0.23	0.12	0.00

*Table B-3. BWE change in depth in inches for bank attached structures.*

<i>Section</i>	<i>1</i>	<i>2</i>	<i>3</i>	<i>4</i>	<i>5</i>	<i>6</i>	<i>7</i>
<i>4-in Vane Spur</i>	0.12	0.12	0.09	0.07	0.05	0.03	0.00
<i>4-in Stream Barb</i>	0.07	0.06	0.05	0.04	0.02	0.01	0.00
<i>8-in Stream Barb</i>	0.21	0.19	0.12	0.10	0.06	0.03	0.00
<i>4-in Three Vanes Sidewall (20 Deg.)</i>	0.13	0.11	0.09	0.07	0.05	0.02	0.00

Table B-4. BWE change in depth in inches for side wall ramp systems.

<b>Section</b>	<b>1</b>	<b>2</b>	<b>3</b>	<b>4</b>	<b>5</b>	<b>6</b>	<b>7</b>
<i>0 Degrees</i>	0.03	0.02	0.02	0.03	0.02	-0.01	0.00
<i>10 Degrees</i>	0.03	0.01	0.02	0.01	0.01	-0.01	0.00
<i>15 Degrees</i>	0.07	0.05	0.04	0.04	0.03	0.01	0.00
<i>20 Degrees</i>	0.10	0.07	0.08	0.06	0.04	0.02	0.00
<i>25 Degrees</i>	0.12	0.09	0.08	0.07	0.04	0.02	0.00

Table B-5. BWE change in depth in inches for boulder system.

<b>Section</b>	<b>1</b>	<b>2</b>	<b>3</b>	<b>4</b>	<b>5</b>	<b>6</b>	<b>7</b>
<i>2 Boulders, 11 Sets</i>	0.21	0.19	0.12	0.10	0.06	0.03	0.00
<i>2 Boulders, 6 Sets</i>	0.06	0.04	0.04	0.03	0.02	0.00	0.00

## B.2 Vertical Mass Transport and Dye Trace Measurements

*Table B-6. VMT data for structures flow conditions of 0.8 ft/s velocity, and 8-inch water depth.*

	<i>Avg, ft.</i>	<i>St. Dev., ft.</i>	<i>Occurrence, %</i>
<i>Clean Flume</i>	16.0	4.5	87
	14.0	4.7	91
<i>Metal Vanes - 1 Set</i>			
1MV(10d)	8.6	2.0	74
3MV(10d)	10.3	2.7	86
5MV(10d)	10.7	3.5	97
1MV(20d) w/ROCKS	9.6	3.4	98
1MV(20d)	7.4	2.2	85
3MV(20d)	7.0	1.9	95
5MV(20d)	6.9	1.9	100
5MV(20d)	6.4	1.8	97
<i>Metal Vanes - 2 Sets (33-in apart)</i>			
1:1MV(20d)	7.4	2.0	98
5:1MV(20d)	7.1	2.2	100
5:3MV(20d)	6.3	2.0	100
5:5MV(20d)	5.6	1.6	100
<i>Boulders</i>			
1B	11.3	3.9	77
1:1B (12-in apart)	11.2	3.8	80
1:1B (33-in apart)	7.8	2.9	99
1:2:1B (12-in apart)	10.9	3.6	85
1:2:1B (cluster)	9.7	3.4	76
2:2B (cluster 45d, 12-in apart)	9.9	3.3	87
<i>Stream Barbs</i>			
4-in Stream Barb - Wall	10.0	2.7	99
4-in Stream Barb - Centerline	9.9	3.5	100
8-in Stream Barb - Wall	10.0	3.9	98

Table B-7. Submergence ratio VMT data for structures flow conditions of 0.8 ft/s and at different water depths.

	<i>Avg, ft.</i>	<i>St. Dev., ft.</i>	<i>Occurrence, %</i>
<i>Depth = 1x, 8-inches</i>			
5MV(20d)	6.9	1.9	100
5MV(20d)	6.4	1.8	97
Clean Flume	16.0	4.5	87
Clean Flume	14.0	4.7	91
<i>Depth = 1.25x, 10-inches</i>			
5MV(20d)	9	2.9	100
5MV(20d)	9.8	2.9	100
Clean Flume	15.8	5.7	100
Clean Flume	17.3	5.3	100
<i>Depth = 1.5x, 12-inches</i>			
5MV(20d)	11.5	3.6	99
5MV(20d)	12.5	3.6	100
Clean Flume	15.7	4.5	100
Clean Flume	16.7	5.5	97